

Drivers of long-term grassland CO₂ fluxes ~~and regrowth~~: effects of management and meteorological conditions ~~over~~ timeduring regrowth periods

5 Yi ~~Wang~~Wang^{1,2}, Iris ~~Feigenwinter~~Feigenwinter¹, Lukas ~~Hörtnagl~~Hörtnagl¹, Anna K. ~~Gilgen~~Gilgen¹,
Nina ~~Buchmann~~Buchmann¹

~~Institute~~¹Institute of Agricultural Sciences, ETH Zurich, 8092 Zurich, Switzerland

²Current address: ICOS ERIC Carbon Portal, Department of Physical Geography and Ecosystem Sciences, Lund University, 22362 Lund, Sweden

Correspondence to: Yi Wang (yi.wang@usys.ethz.ch)

10 **Abstract.** Grasslands serve a unique role in the global carbon (C) cycle and cover about 30% of the European and about 70% of the Swiss agricultural area. Carbon dioxide (CO₂) fluxes of managed grasslands are substantially influenced by land management practices and meteorological conditions, but the temporal development of ~~these drivers~~ isand their effects are still uncertain. ~~With the eddy covariance (EC) technique, net ecosystem CO₂ exchange (NEE) can be directly measured, and then partitioned into gross primary production (GPP; amount of CO₂ fixed through photosynthesis) and ecosystem~~
15 ~~respiration (Reco; amount of CO₂ released via plant and soil respiration).~~ We used 20 years (2005–2024) of ~~EC~~eddy-covariance (EC) fluxes, meteorological data, and detailed management information collected from an intensively managed grassland site (Chamau) in Switzerland, and employed machine learning approaches, i.e., eXtreme Gradient Boosting (XGBoost) models in combination with SHapley Additive exPlanations (SHAP) analyses, to identify drivers and their temporal contributions over two decades. Our study aimed to (1) ~~investigate~~identify intra- and inter-annual variations in
20 grassland CO₂ fluxes, (2) assess magnitude and drivers of gross primary production (GPP) and ecosystem respiration (Reco) during ~~the~~ regrowth periods (i.e., after mowing, grazing, or reseeding), and (3) quantify driver contributions to GPP and Reco over time, with focus on management and extreme events. ~~CO₂ fluxes~~Our results showed pronounced intra- and inter-annual variations in CO₂ fluxes, driven by both management activities as well as meteorological conditions. Despite significant increases in temperature and decreases in soil water content (SWC) during the two decades, GPP and Reco ~~rates~~
25 during regrowth periods remained stable, and no significant trend over time was detected, suggesting adapted, climate-smart decision making of the farmer. The most important drivers of GPP in the long-term were light, management, and temperature, while Reco was mainly driven by temperature, GPP, and management. However, during extreme drought periods in the peak growing ~~season~~seasons (June, July, August), SWC increased in importance and limited GPP. In contrast, the impact of nitrogen (N) fertilization was more differentiated, either acting in parallel with SWC, suggesting low N
30 availability during drought periods, or increasing GPP in years after sward renewal despite low SWC. Overall, our study provided novel insights into relevant drivers of grassland CO₂ fluxes and their complex temporal contributions in the short-

and long-term. Our results suggest that even small climate-smart management adaptations could be promising solutions for stabilizing important grassland processes, such as grassland regrowth, under current and future climate.

35 **Keywords.** Temperate grasslands; climate-smart farming; climate extremes; eddy covariance; driver contributions

1 Introduction

Grassland ecosystems cover 40% of the global ice-free land surface and contribute about one third to the terrestrial carbon (C) stocks (Bai and Cotrufo, 2022; White et al., 2000). Moreover, grasslands provide a broad set of ecosystem services and thus play a unique role in global and regional feed and food production (Henwood, 1998; Richter et al., 2024; Schils et al., 40 2022; Wang et al., 2025b). Temperate permanent grasslands (i.e., grasslands continuously used for forage production, not being part of any crop rotation) account for about 34% of the European and about 70% of the Swiss agricultural ~~areas~~ area (Eurostat, 2020; FSO, 2021). With great capacity to store C belowground and ~~the~~ their large potential to act as a significant C sink, these agroecosystems are often considered as nature-based solutions to mitigate climate change (Bengtsson et al., 2019; Jia et al., 2019). Therefore, accurate understanding and assessment of grassland C dynamics and their drivers are of high 45 relevance to inform grassland management and policies (EASAC, 2022; European Commission, 2023; Soussana et al., 2004; Wang et al., 2019; Xia et al., 2015).

~~As an essential part of the grassland C cycle, carbon~~ Carbon dioxide (CO₂) fluxes at the ecosystem scale are the result of two opposing fluxes: CO₂ uptake as gross primary production (GPP) via plant photosynthesis, and CO₂ release as ecosystem respiration (Reco) via autotrophic and heterotrophic respiration (Reichstein et al., 2005). The balance between these two 50 processes represents the net ecosystem CO₂ exchange (NEE) between the ecosystem and the atmosphere, which can be directly measured at high temporal resolution with the eddy covariance (EC) technique (Aubinet et al., 2012; Eugster and Merbold, 2015). Dynamics of grassland CO₂ fluxes are substantially driven by land management practices (e.g., mowing, grazing, fertilization, sward renewal), climate conditions (e.g., trends, variabilities, and anomalies), and their interactions (Ammann et al., 2007, 2020; Feigenwinter et al., 2023a; Liu et al., 2024; Rogger et al., 2022; Wall et al., 2019, 2020; Winck 55 et al., 2025, 2023; Zeeman et al., 2010). Yet, disentangling their respective effects remains challenging due to high variability across different grassland types, diverse management practices, as well as strong interdependencies and confounding interactions among drivers (Barneze et al., 2022; Chang et al., 2021; Shi et al., 2022).

With ongoing anthropogenic climate change, temperate regions are experiencing rising temperature and atmospheric dryness: (i.e., high vapour pressure deficit (VPD)), reduced precipitation and soil moisture, along with more frequent, 60 intense, and prolonged extreme events such as droughts and heatwaves, and compound extremes (Fischer and Knutti, 2014; Grillakis, 2019; Hermann et al., 2024; IPCC, 2023; Shekhar et al., 2024; Zscheischler et al., 2014). Global meta-analyses showed that warming can promote grassland productivity and increase CO₂ fluxes ~~in general~~ (both GPP and Reco) (Shi et al., 2022; Wang et al., 2019), but temperate grasslands have shown higher sensitivity to warming for Reco compared to GPP

(Wang et al., 2019). In contrast, a latitudinal, cross-site study showed GPP and Reco consistently increased with increasing precipitation but decreased with increasing temperature (Liu et al., 2024). The effect of warming on CO₂ fluxes was also found to interact with management activities such as fertilization (Barneze et al., 2022), mowing or grazing (Shi et al., 2022; Zhou et al., 2019). While extreme events (here mainly droughts, heatwaves, and compound events) typically resulted in reduced magnitude of CO₂ fluxes (Fu et al., 2020; Li et al., 2023a; Reichstein et al., 2013; Zscheischler et al., 2014), their impacts can also be influenced by different management practices. A long-term study comparing intensive and extensive grazing in France found that extensive management may ~~buffer CO₂ fluxes against~~ mitigate the impact of temperature anomalies on CO₂ fluxes (Winck et al., 2025), while another observational study in Switzerland demonstrated that certain management activities could result in higher than usual net CO₂ release, if followed by unfavourable meteorological anomalies (Rogger et al., 2022). Given these diverse findings across spatial and temporal scales and under varying management regimes, it remains difficult to pinpoint the dominant drivers of CO₂ fluxes. ~~Moreover, scientific evidence is urgently needed to determine which management~~ identify and recommend climate-smart agricultural practices should be recommended to adapt to or to mitigate, as requested by international institutions (FAO, 2019; World Bank, 2024), which allow for mitigating future climate risks and improving resilience in grassland-based farming systems. (Lipper et al., 2014; Walter et al., 2017).

Long-term field studies using the EC technique have been able to capture the temporal variability of CO₂ fluxes with additional consideration of actual management activities (Ammann et al., 2020; Feigenwinter et al., 2023a; Rogger et al., 2022; Winck et al., 2025); Wohlfahrt et al., 2008). However, current studies evaluating the drivers of CO₂ fluxes have typically used traditional linear models to ~~analyze~~ analyse the effects of climate conditions, only sometimes considering also management practices. ~~Linear~~ However, linear models frequently fail to capture ~~the~~ non-linear, interactive, and highly dynamic nature variable effects of drivers that influence CO₂ fluxes in complex systems such as intensively managed agroecosystems (Feigenwinter et al., 2023b; Maier et al., 2022). As In contrast, a powerful alternative, are machine learning models, which are capable of integrating these complex drivers at high temporal resolution and can account for management events. Although these models operate as black boxes, providing only aggregated measures of driver importance, advancements in interpretable machine learning such as SHapley Additive exPlanations (SHAP) analysis (Lundberg et al., 2020; Lundberg and Lee, 2017) now enable the estimation of individual driver contributions and importance for each discrete observation. This capability allows the attribution of CO₂ flux variability and facilitates the identification of temporal changes in underlying drivers. In this study, we present 20 years (2005–2024) of CO₂ fluxes measured at an intensively managed temperate grassland in Switzerland. Using additional meteorological data and well-documented management information, we applied eXtreme Gradient Boosting (XGBoost) models in combination with SHAP analysis to address the following objectives: (1) ~~investigate~~ identify intra- and inter-annual variations in grassland CO₂ fluxes, (2) assess magnitude and drivers of GPP and Reco during ~~the~~ regrowth periods (i.e., after mowing, grazing, or reseeded), and (3) quantify driver contributions to GPP and Reco over time, with focus on management and extreme events.

2 Material and methods

2.1 Study site

The study site Chamau is a permanent grassland located in the canton of Zug, Switzerland (47°12'36.8" N and 8°24'37.6" E, 393 m a.s.l.). In 2005, an eddy covariance EC and meteorological station (part of FLUXNET as CH-Cha) was established, and CO₂ and H₂O vapour fluxes have been continuously measured since then. The average annual temperature ~~is~~was 9.9 °C, and the average annual precipitation sum ~~is~~was 1147 mm over the study period (2005–2024). The soil of the grassland parcels surrounding the flux station is classified as a Cambisol/Gleysol and has a silt loam soil texture, with a pH of 5.3 in the topsoil (Roth, 2006). This grassland ~~is~~has been intensively managed, with four to six mowing events per year, occasional grazing by sheep, and organic fertilizer application (mainly as slurry, normally applied once after each mowing event, on average 260 kg N ha⁻¹ yr⁻¹ from 2005 to 2024). In February 2012 and August 2021, the sward was renewed, i.e., the existing sward was ~~destroyed~~terminated and ploughed, and a new sward was sown. The vegetation in the grassland includes English ryegrass (*Lolium perenne*), common meadowgrass (*Poa pratensis*), Italian ryegrass (*Lolium multiflorum*), white clover (*Trifolium repens*), red clover (*Trifolium pratense*), and dandelion (*Taraxacum officinale*) (Feigenwinter et al., 2023a).

2.2 Management information and regrowth periods

The Chamau grassland site consists of two parcels A and B (Feigenwinter et al., 2023a), and detailed management information from this site has been continuously documented since 2005, including major activities like mowing, grazing, fertilization, and sward renewal. ~~A~~A nitrous oxide (N₂O) mitigation experiment was carried out from 2015 to 2020, where parcel A received standard fertilization, while parcel B was oversown with a higher legume proportion and received no fertilization (Feigenwinter et al., 2023b; Fuchs et al., 2018). Since parcel B dominated the footprint area in earlier years (2005–2013; Fig. B3 in Feigenwinter et al., 2023a), and the two parcels were under similar mowing and grazing scheme ~~in recent years~~, during the entire study period (Tab. B2 in Feigenwinter et al., 2023a; Tabs. A4, A5), we adopted the management scheme of parcel B to define regrowth periods in the current study.

We defined the period between two mowing/grazing/sward renewal events as a regrowth period (excluding the day(s) when management occurred). Each regrowth period consists of a minimum of ten days. ~~This allowed us to consider slightly different~~If several management activities ~~on both parcels~~took place only a few days apart within the entire footprint, we ~~defined the latest activity~~ as ~~on~~the start of the next regrowth period. For example, in earlier years, the parcels were occasionally first partially grazed and then partially mowed within a certain time window, ~~or vice versa~~. We thus considered ~~such management patterns~~the start date of the grazing as ~~on~~the end of the previous regrowth period, and the mowing date as the beginning of the next regrowth period. A 'DaySinceUse' variable was generated for each day in a regrowth period to indicate numbers of days since the last mowing/grazing/sward renewal event. An average daily fertilizer nitrogen (N) input for each regrowth period (DailyN, in kg N ha⁻¹ day⁻¹) was calculated based on the total fertilizer N received during the period and the length of that period. If parcel A and B had different N inputs for certain regrowth periods, the average of the two

parcels was used as the total N input. ~~For GPP and Reco during each regrowth period, CO₂ fluxes, i.e., GPP and Reco~~
130 ~~regrowth rates~~ (in g C m⁻² day⁻¹), were calculated based on the cumulative CO₂ uptake ~~or~~ release over the regrowth period
(in g C m⁻²) divided by the length of the regrowth period (i.e., number of days). If the ~~middle date~~ center of ~~one~~ regrowth
~~period~~ periods was between April and September ~~(which is, i.e., the main growing season), the period was for agricultural~~
~~grasslands in central Europe, they were~~ classified as a spring-summer ~~period~~ regrowth periods, else as an autumn-winter
~~period~~ regrowth periods.

135 2.3 Flux and meteorological measurements and data processing

Since July 2005, molar densities of CO₂ and H₂O vapour were measured with open path infrared gas ~~analyzers~~ analysers
(IRGAs; LI-7500; LI-COR Biosciences, USA) at 2.42 m measurement height ~~and tilted 15° from the vertical~~, together with
measurements of 3D wind speed and wind direction using ultrasonic anemometers (R3-50, Gill Instruments Ltd., UK) at 20
Hz time resolution. Meteorological variables, including air temperature (TA, in °C), relative humidity (RH, in %),
140 ~~air~~ atmospheric pressure (PA, in hPa), incoming and outgoing shortwave and longwave radiation (SW IN/OUT and LW
IN/OUT, in W m⁻²), incoming and outgoing photosynthetic photon flux density (PPFD IN/OUT, in μmol m⁻² s⁻¹),
precipitation (PREC, in mm), soil temperature (TS, in °C), and ~~volumetric~~ soil water content (SWC, %), were also measured.
For ~~detailed~~ more details on instrumentation, see Feigenwinter et al. (2023a).

Half-hourly CO₂ and H₂O vapour fluxes were calculated with EddyPro (v7.0.9) based on the covariance of the turbulent
145 fluctuations of gas concentration and vertical wind speed. Widely used community guidelines, ~~(Aubinet et al., 2012;~~
~~Pastorello et al., 2020, Sabbatini et al., 2018)~~, including corrections for density fluctuations (Webb et al., 1980), double axis
rotation (Wilczak et al., 2001), high-pass (Moncrieff et al., 2005) and low-pass filtering effects (Horst, 1997), were applied.
~~Time lags were detected using covariance maximization in a small~~ The default self-heating correction for the open path LI-
7500 (Burba et al., 2008) was not applied because it was developed specifically for vertically mounted IRGAs, and applying
150 ~~it to a 15°-tilted setup without a parallel reference flux for validation would risk introducing systematic over-corrections,~~
~~larger than the random uncertainty of the measurement (Deventer et al., 2021). Time lags were detected using covariance~~
~~maximization in a short~~ time window (between 0.05 s and 0.55 s), with a default time lag (typically 0.30 s) if no clear time
lag was found. Post-processing for quality assessment and gap-filling was done in the Python library diive (Hörtnagl, 2025a),
NEE flux partitioning into GPP and Reco ~~based on the night-time method (Reichstein et al., 2005)~~ was done with the R
155 package REdDyProc (v1.3.3, Wutzler et al., 2018). During quality assessment, a series of quality control flags were applied
to classify data quality (after testing steady-state, data completeness, spectral correction factor, IRGA signal strength, outlier
detection), and turbulence-based constant friction velocity (USTAR) thresholds ~~were applied~~ (0.05, 0.07, and 0.09 m s⁻¹ for
the 16th, 50th, and 84th percentile of the USTAR threshold distribution, ~~respectively~~) ~~were applied~~. An overall Quality
Control Flag (QCF) was generated, ~~integrating all assessments to filter for high quality data. Resulting data gaps were then~~
160 filled using random forest models utilizing a sliding three-year window for annual model training (Breiman, 2001; Hörtnagl,
2025a). For all ~~our analysis~~ further analyses, we used quality-controlled fluxes that were filtered with the 50th percentile of

the USTAR threshold distribution, subsequently gap-filled using random forest models, and partitioned into GPP and Reco [based on the night time method \(Reichstein et al., 2005\)](#).

For meteorological data, a similar quality assessment procedure was applied with the diive library (Hörtnagl, 2025a), and all screened variables were aggregated into half-hourly resolution. Vapour pressure deficit (VPD) was calculated based on TA and RH. For [soil temperature](#) TS (at 0.04 m, 0.15 m, and 0.4 m depths) and [soil water content](#) SWC (at 0.05 m, 0.15 m, and 0.75 m depths) measurements, averages across all depths were calculated and used in the final analysis-

[to represent the overall soil conditions over the entire soil profile](#). All data used in this study were derived from the most recent PI dataset (Hörtnagl et al., 2025), with all processing steps openly documented in a GitHub repository (Hörtnagl, 2025b).

2.4 Data [analysisanalyses](#)

2.4.1 Trend analysis, extreme detection, and functional relationships

To detect monotonic trends in monthly and yearly meteorological variables, we applied the Mann-Kendall test (Kendall, 1955; Mann, 1945). If the temporal trend was significant (p -value < 0.05), we additionally obtained the slope and sign of the trend with Sen's slope estimator (Sen, 1968). We tested trends in GPP and Reco across all regrowth periods, ~~moreover~~. [Moreover](#), two seasons were ~~tested~~[compared](#) as well: spring-summer (April to September) and autumn-winter (October to March).

To identify months with high soil and air dryness, z-scores were calculated for monthly average SWC and VPD using ~~the~~ equation [1](#):

$$z = \frac{x - \mu}{\sigma} \quad (1)$$

where x represents the monthly average for SWC or VPD, μ is the respective overall mean, and σ is the respective standard deviation for all monthly values across the entire study period. Months with z-scores for SWC lower than minus two were defined as [months with](#) high soil dryness, and months with z-scores of VPD higher than two were defined as [months with](#) high air dryness.

To evaluate the functional relationship between PPFD and GPP, we assigned regrowth periods to three categories, i) two years before (i.e., 2010 and 2011; 2019 and 2020) and ii) two years after (i.e., 2013 and 2014; 2022 and 2023) the grassland renewal years (2012 and 2021), and iii) all remaining years ~~without~~[excluding](#) the renewal years. Second degree polynomial regressions were then fitted using the average PPFD (calculated from the daily total PPFD) and GPP ~~regrowth rates across~~ [during](#) regrowth periods ([see Section 2.2](#)) within each category.

2.4.2 XGBoost models and SHAP [analysisanalyses](#)

To model effects of different drivers on daily GPP and Reco (in $\text{g C m}^{-2} \text{ day}^{-1}$), we applied two eXtreme Gradient Boosting (XGBoost) models (Chen and Guestrin, 2016), one model for GPP and one model for Reco, based on 20 years of data. For

GPP, we selected management indicators (i.e., DaySinceUse and DailyN) and major meteorological variables (i.e., PPF, TA, TS, PREC, SWC, and VPD) as predicting features. For Reco, TS was used instead of TA, and GPP was added as an additional feature: [to better represent the C supply and C allocation for autotrophic and heterotrophic respiration](#). Input daily data from all 20 years were randomly split into 70% and 30% for training and testing datasets, respectively. Major hyperparameters (i.e., number of estimators, max depth, learning rate, and subsample) in both XGBoost models were fine-tuned using grid search with 10-fold cross-validation to improve performance and avoid overfitting. The best hyperparameters that minimized root mean ~~squared~~ error (RMSE) were then used in the final models (Table Tab. A1).
To evaluate model performance and generalization on the testing dataset, metrics like ~~root mean square error~~ (RMSE) and the coefficient of determination (R^2) were calculated.

To estimate the marginal contribution (i.e., SHAP value) of each feature to every model prediction (here, daily GPP and Reco predictions), we used the TreeExplainer SHAP framework that was designed specifically for tree-based ensembles like XGBoost (Lundberg et al., 2020). SHAP values at zero represent the overall mean prediction of the background dataset, which is a collection of representative data points used to estimate the expected model output that SHAP compares individual predictions against (Lundberg et al., 2020; Molnar, 2023). ~~The SHAP value of~~ a feature (i.e., a driver variable) ~~has a~~ [represents the effect of that driver, at its specific value, on each individual prediction](#). A positive SHAP value, [indicates that](#) this ~~feature~~ [driver](#) increases the local prediction ~~relative~~ [compared](#) to the overall mean prediction, and vice versa ~~for negative SHAP values~~. Higher absolute SHAP values represent larger ~~impact~~ [effects](#) (positive or negative) on predicted fluxes. For each prediction (here, daily GPP and Reco), the sum of all SHAP values across all features equals the difference between the local model prediction (i.e., the predicted fluxes) and the overall mean prediction (from the background dataset), which is consistent with the additive property of SHAP values (Gou et al., 2024; Krebs et al., 2025; Qiu et al., 2022). ~~In this study, we performed two SHAP analyses (1 and 2) with different foci.~~ [The relationship between each driver and its SHAP values was further explored using SHAP dependence plots.](#)

[In this study, we performed two SHAP analyses \(1 and 2\), based on the same XGBoost model for daily CO₂ fluxes, but with different foci:](#)

SHAP analysis 1: For a general comparison, the “tree_path_dependent” method was used as feature perturbation method. Thus, the mean prediction at SHAP zero represents roughly the mean prediction (i.e., [of](#) GPP or Reco) of the training dataset. We then averaged [the](#) daily SHAP values [of any given feature](#) for each regrowth period. ~~The mean of all SHAP values for one feature in a certain regrowth period was calculated~~ to ~~represent an~~ [calculate the](#) average effect of that feature on [the](#) predicted fluxes during ~~this~~ [the regrowth](#) period.

SHAP analysis 2: To evaluate the ~~impact~~ [effect](#) of ~~different~~ [relevant](#) drivers on daily GPP during ~~the~~ extreme months (~~detected in previous steps~~), we used the “interventional” method as feature perturbation method (Lundberg et al., 2020). [Thus](#) [With this method](#), SHAP values can be calculated that compare the predictions to a certain subset of samples (Molnar, 2023). Here, we used only the months during the peak growing ~~season~~ [seasons](#) (June, July, August) when no extreme weather conditions occurred as the background dataset ~~and~~. [We](#) then calculated a second set of SHAP values for ~~only~~ the peak

growing ~~season~~ seasons in 2018, 2019, 2022, and 2023, as these times included the majority of recent extreme months. With this approach, we ~~also~~ eliminated the impact of seasonality in the data and ~~assessed only~~ were able to assess the impact of extreme events ~~only~~.

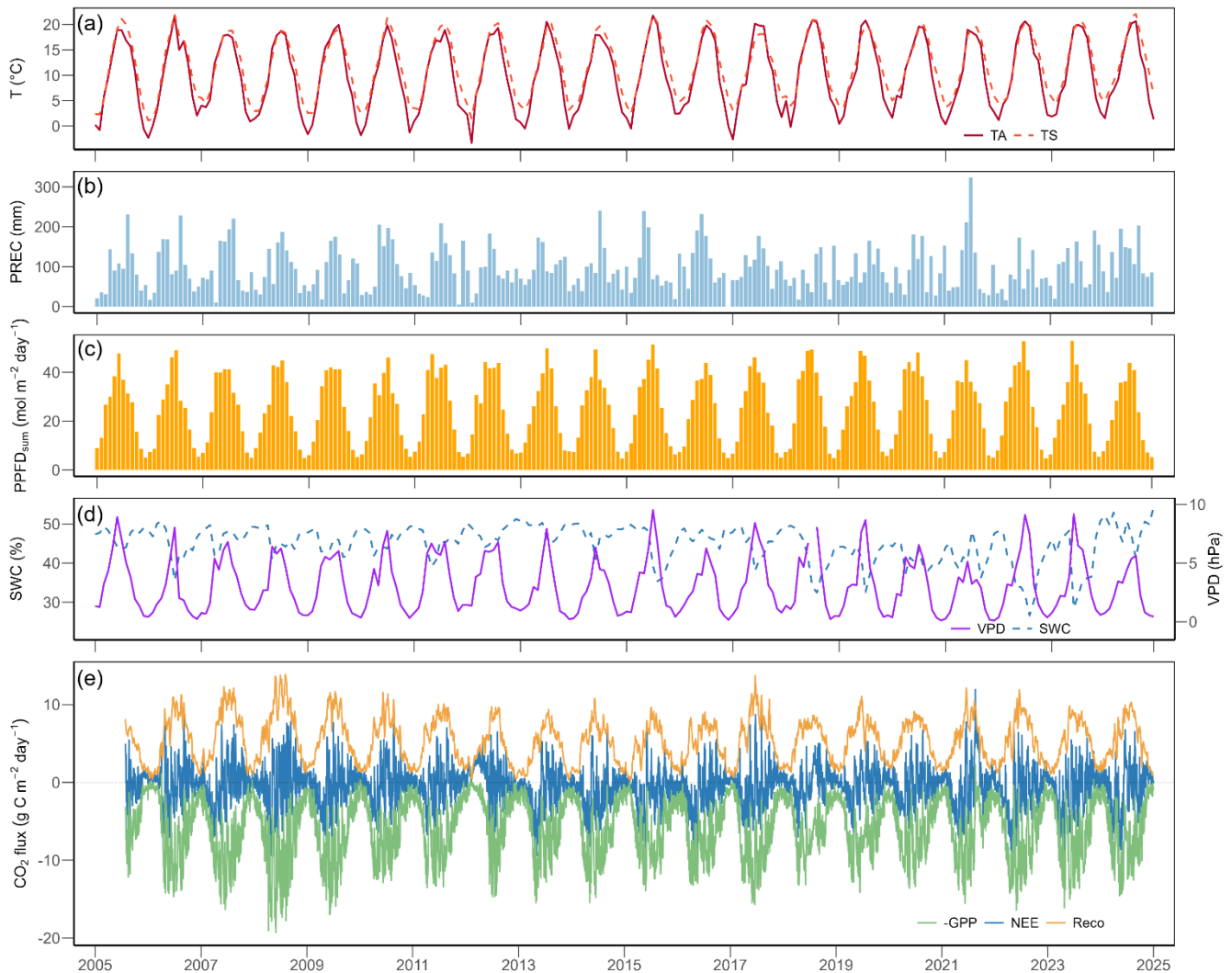
230 XGBoost models and SHAP analyses were performed in Python (version 3.11.11, Python Software Foundation, 2024) using the libraries xgboost (v3.0.0, Chen and Guestrin, 2016), shap (v0.47.1, Lundberg and Lee, 2017), and scikit-learn (v1.6.1, Pedregosa et al., 2011). Other statistical analyses and visualization were done in R version 4.4.1 (R Core Team, 2024).

3. Results

3.1 Meteorological conditions and CO₂ fluxes over 20 years

235 During the past 20 years (2005–2024), the Chamau grassland experienced a mild temperate climate, ~~with mean annual air temperature of (MAT 9.9 °C and mean annual precipitation of, MAP 1147 mm-)~~. At an annual scale, ~~air temperature~~TA at this site increased significantly by 0.071 °C yr⁻¹ (Mann Kendall test $p < 0.01$), mean ~~soil temperature~~TS and minimum ~~soil temperature~~TS also increased by 0.070 °C yr⁻¹ and 0.095 °C yr⁻¹, respectively ($p < 0.01$). The years 2018 and 2022 were the hottest years on record, with mean annual ~~air temperature~~TA of 11.0 °C and 11.1 °C, respectively, while the years 2010 and
240 2013 were the coldest years, with mean annual ~~air temperature~~TA of 8.6 °C and 9.0 °C, respectively. Annual ~~precipitation~~PREC did not show a significant trend ($p = 0.87$) over the 20 years. Nevertheless, the years 2018 and 2022 were the driest years on record, with annual ~~precipitation~~PREC of 906 mm and 884 mm, respectively, while the years 2016 and 2024 were the wettest years, with annual ~~precipitation~~PREC of 1351 mm and 1378 mm, respectively.

At the monthly scale, meteorological conditions showed pronounced seasonal variability (Fig. 1a-d). Overall, monthly ~~air~~TA
245 ~~temperature~~TA reached maximum values in July (mean of 19.6 °C) and minimum values in January (mean of 1.0 °C). Monthly ~~air temperature~~TA (Fig. 1a), ~~precipitation~~PREC (Fig. 1b), and VPD (Fig. 1d) did not show significant trends over time ($p = 0.21$ for TA, $p = 0.69$ for PREC, $p = 0.51$ for VPD), while ~~soil water content~~SWC (Fig. 1d) decreased significantly over the 20 years (slope = -0.016 % month⁻¹, $p < 0.01$). Looking at each specific month (i.e., across 20 years), ~~air~~TA and ~~soil~~TS
250 ~~temperature~~TS increased significantly in the winter months (December to March; ~~Table 1~~Tab. A2). August was the only month to experience a decrease in ~~precipitation~~PREC, which otherwise remained stable. ~~Soil water content~~SWC significantly decreased in late summer and autumn (August to October; ~~Table 1~~Tab. A2). Based on the z-scores, four months of extreme air dryness, seven months of extreme soil dryness, and six months of compound extremes (i.e., high VPD and low SWC) were identified (Fig. 2). These extreme conditions mainly occurred between May and September, particularly during the peak growing season months (June, July, and August) in the years 2018, 2019, 2022 and 2023.



255

Figure 1. Meteorological variables and CO₂ fluxes at the Chamau grassland site from 2005 to 2024: (a) monthly mean air temperature (TA, red solid line) and soil temperature (TS, orange dashed line), (b) monthly sum of precipitation (PREC), (c) monthly mean daily total photosynthetic photon flux density (PPFD_{sum}), (d) monthly mean volumetric soil water content (SWC, blue dashed line) and vapour pressure deficit (VPD, purple solid line), (e) daily sum of net ecosystem CO₂ exchange (NEE, blue line), gross primary production (GPP, green line), and ecosystem respiration (Reco, orange line).

260

Daily NEE, GPP, and Reco showed strong interannual and seasonal variations over the 20 years (Fig. 1e, [Table A2/Tab. A3](#)). Annual cumulative NEE ranged from 140 g C m⁻² yr⁻¹ (in 2012) to -503 g C m⁻² yr⁻¹ (in 2014), with an overall mean (\pm standard deviation) of -260 (\pm 172) g C m⁻² yr⁻¹ (Fig. A1). In 2012 and 2021, two grassland renewal events (i.e., ploughing and reseeded of the grassland) took place, with very different effects on annual NEE: while the event in 2012 led to a strong net CO₂ loss (cumulative NEE of 139 g C m⁻² yr⁻¹; Fig. A1), the event in 2021 resulted only in a weaker-than-normal net CO₂ uptake (cumulative NEE of -163 g C m⁻² yr⁻¹; Fig. A1). All three flux components were strongly influenced by

265

management practices (Fig. A2, Table A3, 3a, Tabs. A4, A5) such as mowing and grazing. Strongest net CO₂ uptake occurred in early spring (March-April), while the largest net CO₂ release happened in early winter (December-January).

Table 1. Monthly meteorological variables from 2005 to 2024. For each month, mean and standard deviation, trends (unit yr⁻¹; in red positive trends, in blue negative trends) and significance from Mann-Kendall test (p values < 0.05: *, < 0.01: **) are shown.

Variable	Unit	Jan		Feb		Mar		Apr	
		Mean±SD	Trend	Mean±SD	Trend	Mean±SD	Trend	Mean±SD	Trend
TA_mean	°C	0.96±1.95		1.84±2.41	0.2*	5.26±1.3		9.48±1.36	
TA_min	°C	-10.22±3.58		-8.96±3.74		-6.48±3.03	0.253*	-3.05±1.56	
TA_max	°C	12.45±3.36		15.01±3.48		19.8±2.26		24.35±2.33	
TS_mean	°C	3.9±1.23	0.144**	3.79±1.48	0.164**	6.16±1.18	0.121*	10.07±0.73	
TS_min	°C	2.24±1.05	0.096**	1.97±1.14	0.11**	3.43±1.47	0.141*	6.49±1.27	
TS_max	°C	6.15±1.56	0.162*	6.33±1.57	0.162*	9.81±1.34		13.84±1.54	
PREC_sum	mm	64.28±35.59		48.81±23.57		65.68±34.35		83.51±48.92	
SWC_mean	%	48.19±2.19		48.07±2.16		47.65±2.99	-0.236*	45.15±3.85	
SWC_min	%	46.21±2.49		46.3±2.94		45.39±3.51	-0.302*	41.08±4.96	
SWC_max	%	49.76±2.19		49.57±2.25		49.07±2.47		46.77±4.01	
VPD_mean	hPa	0.73±0.36		1.2±0.39		2.36±0.61		3.8±1.17	
VPD_max	hPa	6.55±2.02	-	10.13±3.51	-	15.6±3.16	-	21.28±4.9	-

Table 1. (continued)

Variable	May		Jun		July		Aug	
	Mean±SD	Trend	Mean±SD	Trend	Mean±SD	Trend	Mean±SD	Trend
TA_mean	13.77±1.51		18.1±1.11		19.55±1.35		18.61±1.45	0.157**
TA_min	1.47±2.08		5.9±1.64		8.41±1.37		7.56±1.09	
TA_max	28.18±2.56		32.28±1.93		33.71±1.7		32.42±2.63	
TS_mean	13.83±1.06		17.91±1.07		20.08±1.15		19.62±1.04	0.092*
TS_min	10.58±1.14		14.02±1.39		17.1±0.8		16.85±1	
TS_max	17.73±1.83		22.1±1.99		23.5±1.92		22.91±1.67	
PREC_sum	135.84±49.35		140.56±52.47		148.2±71.1		142.83±46.43	-4.057*
SWC_mean	44.46±3.89		42.78±5.34		42.17±5.83		41.74±5.69	-0.468*
SWC_min	39.28±4.92		38.13±5.85	-0.356*	37.16±5.45		37.25±5.69	
SWC_max	45.94±3.97		44.66±5.25		44.34±5.37		44.29±5.02	
VPD_mean	4.5±1.26		6.21±1.41		6.9±1.69		5.43±1.4	
VPD_max	25.57±4.74	=	32.02±4.52	=	35.82±6.37	=	29.97±7.05	=

Table 1. (continued)

Variable	Sep		Oct		Nov		Dec	
	Mean±SD	Trend	Mean±SD	Trend	Mean±SD	Trend	Mean±SD	Trend
TA_mean	14.91±1.4		10.36±1.32		5.01±1.06		1.54±1.44	
TA_min	3.72±1.65		0.26±2.49		4.75±3.01	0.252*	8.73±3.91	
TA_max	28.4±1.76		23.56±2.28		16.96±2.84		12.41±1.98	
TS_mean	16.96±1.03		13.41±0.81		9.02±1.12	0.102*	5.41±1.24	0.123**
TS_min	13.91±1.17		10.46±1.57	0.128*	6±1.79	0.18*	3.69±1.2	0.174**
TS_max	20.35±1.79		16.46±1.05		12.1±1.2		7.54±1.36	0.119*
PREC_sum	93.18±44.69		76.67±28.61		66.45±44.14		81.25±44.07	
SWC_mean	42.43±5.16	-0.44*	43.79±4.26	-0.399*	45.74±3.34		47.72±3.05	
SWC_min	38.64±5.09	-0.538*	40.98±4.64		43.62±3.41		45.86±3.07	
SWC_max	44.85±4.57	-0.351*	46.01±3.8	-0.306*	47.33±3.31		49.24±3.02	
VPD_mean	3.28±0.65		1.54±0.52		0.76±0.37	-0.032*	0.53±0.34	
VPD_max	21.64±3.8	=	14.92±4.08	=	8.48±2.87	=	5.51±1.27	=

275

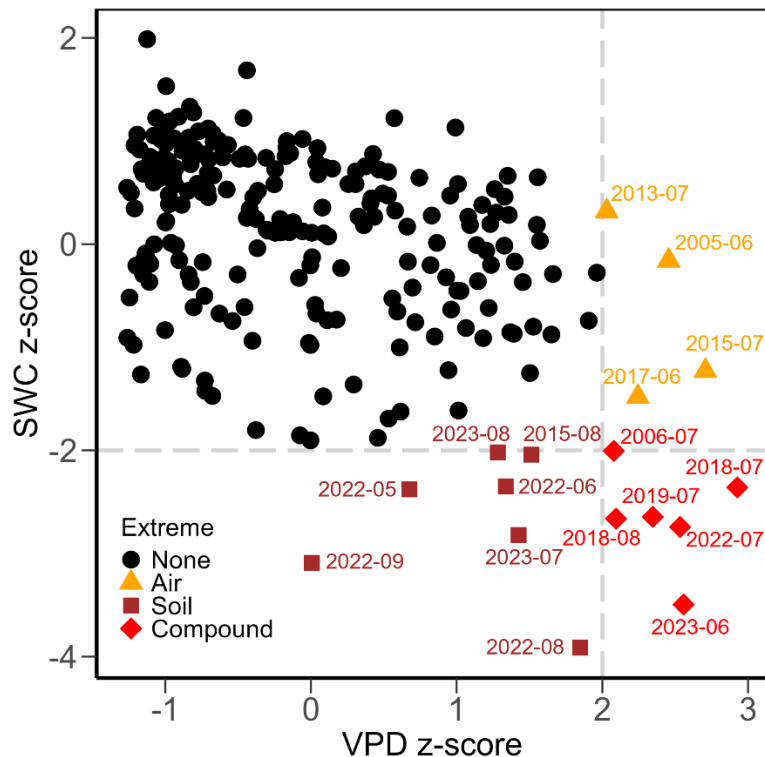
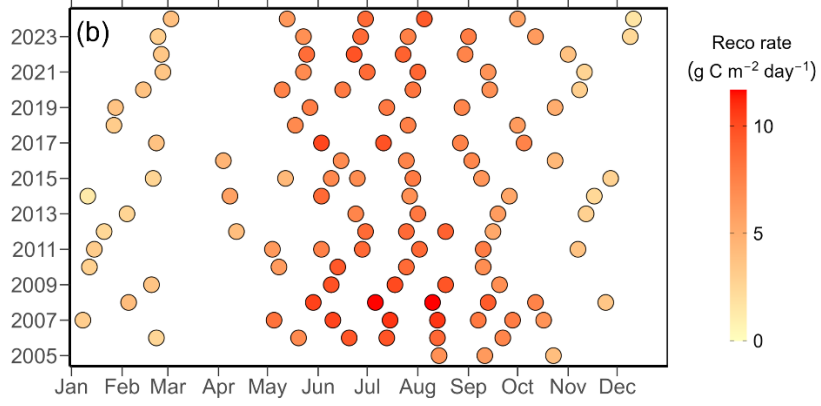
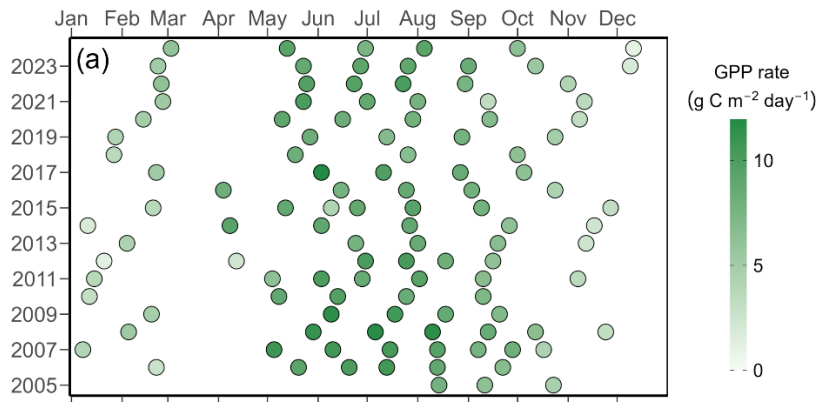


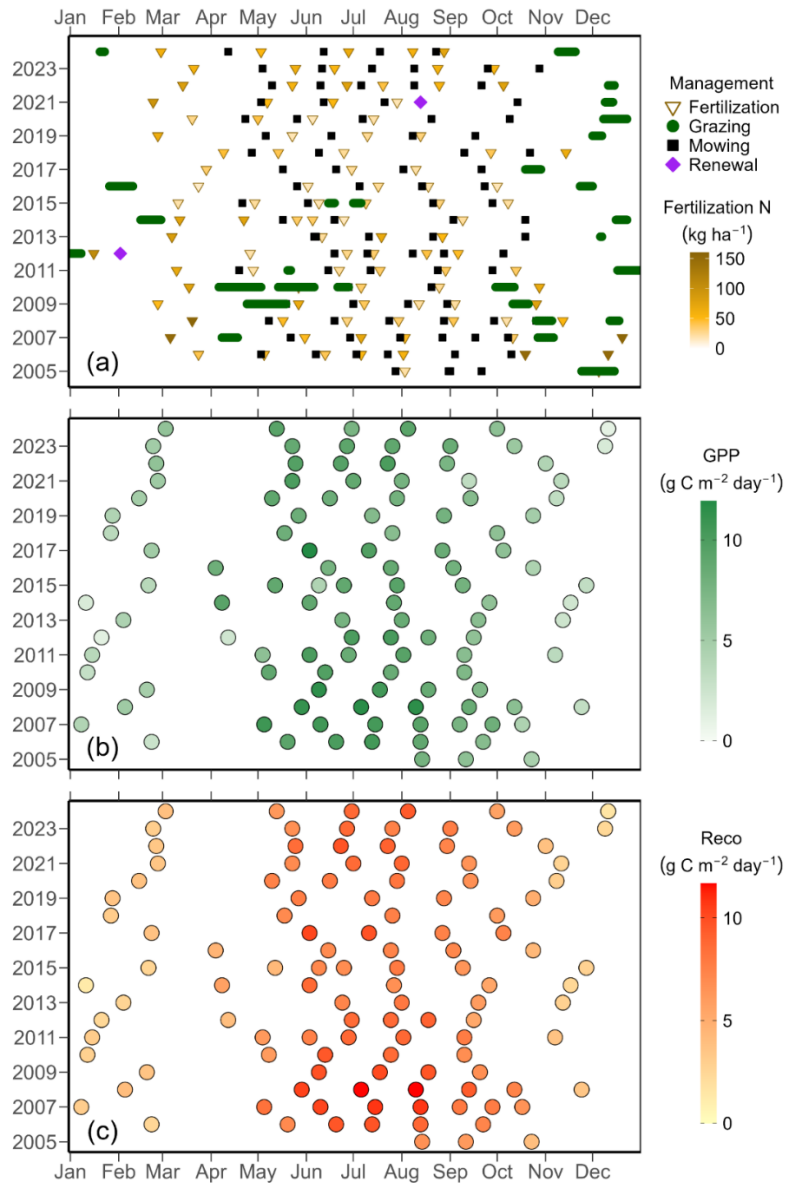
Figure 2. Z-scores for monthly mean vapour pressure deficit (VPD) and volumetric soil water content (SWC) from 2005 to 2024. Grey dashed lines indicate thresholds for extreme months (z-score of 2 for VPD and of -2 for SWC). Symbols and colours indicate types of extreme: none (black dots), high air dryness (orange triangles), high soil dryness (dark red squares), and compound air and soil dryness (red diamonds).

280

3.2 Management and CO_2 fluxes during regrowth ~~rates~~ periods

The Chamau grassland was managed intensively during the past two decades, and experienced in total 94 mowing events, 319 days of grazing, and 102 fertilizer applications. Moreover, the grassland was renewed twice, in 2012 and 2021 (Fig. A23a). This resulted in 115 grassland regrowth periods during the 20 years of this study. ~~Overall, mean~~ The average (\pm standard deviation) ~~GPP~~ length of the regrowth ~~rate~~ period was $7.2 (\pm 2.6) \text{ g C m}^{-2} \text{ day}^{-1}$ and ~~Reco~~ $58 (\pm 47)$ days, with shorter regrowth ~~rate~~ was $6.6 (\pm 2.5) \text{ g C m}^{-2} \text{ day}^{-1}$ (Fig. 3). ~~periods in spring-summer seasons (39 ± 20 days) and longer regrowth periods in autumn-winter seasons (100 ± 60 days).~~ During spring ~~and~~ summer seasons (i.e., April to September), about four mowing/grazing events took place (about two to three events in extreme dry years of 2018 and 2019), ~~with a typical~~. A slightly increasing trend ($p = 0.01$) was found for the length of regrowth ~~period of about 39 days.~~ The average GPP ~~periods~~ over the 20 years of the study: While the length of regrowth ~~rate~~ periods during the spring-summer seasons ~~was increased significantly ($p < 0.01$), no significant trend was found during the autumn-winter seasons ($p = 0.87$).~~ Generally, longer regrowth periods corresponded to lower GPP and Reco. Overall, mean (\pm standard deviation) GPP during regrowth periods was $7.2 (\pm 2.6) \text{ g C m}^{-2} \text{ day}^{-1}$ and Reco during regrowth periods was $6.6 (\pm 2.5) \text{ g C m}^{-2} \text{ day}^{-1}$ (Fig. 3b-c). The average GPP and Reco during regrowth periods in spring-summer seasons were $8.6 (\pm 1.4) \text{ g C m}^{-2} \text{ day}^{-1}$, ~~while Reco regrowth rate averaged and~~ $7.9 (\pm 1.6) \text{ g C m}^{-2} \text{ day}^{-1}$. ~~During, respectively. In comparison, average GPP and Reco in~~ autumn-winter seasons, ~~regrowth rates~~ were ~~lower, with~~ $4.1 (\pm 1.4) \text{ g C m}^{-2} \text{ day}^{-1}$ for GPP and $3.7 (\pm 1.5) \text{ g C m}^{-2} \text{ day}^{-1}$ for Reco, ~~respectively.~~ We did not observe any significant trend for GPP ~~during regrowth rates~~ periods over the 20 years (overall $p = 0.13$), regardless of seasonality (spring-summer season: $p = 0.10$; autumn-winter season: $p = 0.33$). Similarly, Reco ~~during regrowth rates~~ periods did not change significantly over time (overall $p = 0.07$), ~~nor~~ not during the spring-summer ~~season~~ ($p = 0.08$) ~~nor~~ the autumn-winter ~~season~~ seasons ($p = 0.84$).





305 **Figure 3. Management events (a) and CO₂ fluxes (b-c) during regrowth periods. (a) Major management events at the Chamau**
grassland site between July 2005 and December 2024. The x-axis position of each point indicates the date of each event. Symbols
represent different management activities: fertilization (brown triangles), mowing (black squares), grazing (green circles), and
sward renewals (purple diamonds). Colours of fertilization triangles represent the amount of nitrogen inputs, with darker colours
meaning higher inputs. Flux rates CO₂ fluxes for (ab) gross primary production (GPP) and (bc) ecosystem respiration (Reco) for
individual regrowth periods between 2005 and 2024. Points indicate the regrowth rates over a given GPP or Reco during a
regrowth period, with the x-axis position corresponding to the midpoint date center of that period. Darker colours represent high
regrowth rates GPP or Reco values.
 310

3.3 Drivers of GPP and Reco

3.3 Drivers of GPP and Reco

The XGBoost models for daily GPP and Reco performed well (Fig. [A3A2](#)), with a RMSE for GPP of 1.2 g C m⁻² day⁻¹ and an R² of 0.91 on the testing set (Fig. [A2a](#)). The performance of the Reco models was better, with a RMSE of 0.6 g C m⁻² day⁻¹ and R² of 0.96 on the testing set (Fig. [A3a](#)). The performance of the Reco models was better, with a RMSE of 0.6 g C m⁻² day⁻¹ and R² of 0.96 on the testing set (Fig. [A3eA2c](#)). The three most important drivers for daily GPP were PPFD, TS, and DaySinceUse (Fig. [A3bA2b](#)), while the three most important drivers for daily Reco were TS, GPP, and DailyN (Fig. [A2d](#)). For both GPP and Reco, the drivers showed strong seasonality over the 20 years of the study (Fig. 4; SHAP analysis 1). [A3d](#).

~~For both GPP and Reco, the drivers showed strong seasonality over the 20 years of the study (Fig. 4; SHAP analysis 1).~~ PPFD and temperature normally increased GPP ~~relative to the mean~~ in summer compared to the overall mean, while low light and low temperature conditions in winter decreased GPP ~~from~~compared to the mean (Fig. 4a). At daily scale, higher PPFD (Fig. A3a) and higher TS (Fig. A3b) had more positive effects on GPP than lower PPFD and lower TS (i.e., SHAP values of both drivers generally increased (and then saturated for TS) with increasing magnitude of the driver values). When averaged over the entire regrowth period, management events (i.e., mowing and grazing, represented by DaysSinceUse) typically had a negative effect (i.e., negative SHAP values) on GPP compared to the overall mean GPP (Fig. 4a). However, at daily scale (Fig. A3c), SHAP values for DaySinceUse were first negative, but then steadily increased towards positive before becoming stable after around 20 days, indicating that GPP increased the more time had passed since the last management event. Compared to the main drivers of GPP (light, temperature, and management), water-related drivers (i.e.,

~~Compared to the main drivers of GPP (light, temperature, and management), water-related drivers (i.e., SWC, VPD, and PREC) had a relatively smaller contribution~~contributions and showed a less strong seasonality. However, during the extreme summers (i.e., 2018, 2019, 2022, and 2023), especially SWC increasingly limited GPP (negative SHAP values compared to normal years). The main drivers of Reco, i.e., ~~The main drivers of Reco, i.e., temperature~~TS and GPP, showed a similar seasonality, with higher ~~soil temperature~~TS and higher GPP in summer generally promoting respiration, while in winter, these drivers limited Reco (Fig. ~~4b~~4b). At daily scale, the effects of these two drivers on Reco became more positive with higher TS (Fig. A3d) and higher GPP (Fig. A3f). Compared to the drivers of GPP, fertilizer N inputs were more important for Reco than DaySinceUse, while water-related drivers had relatively low importance and ~~low impacts~~smaller effects on Reco. ~~Negative effects of SWC on Reco during~~During the extreme summers when low SWC occurred, negative effects of SWC on Reco were more obvious in 2022 and 2023 compared to earlier years (e.g., 2018 and 2019).

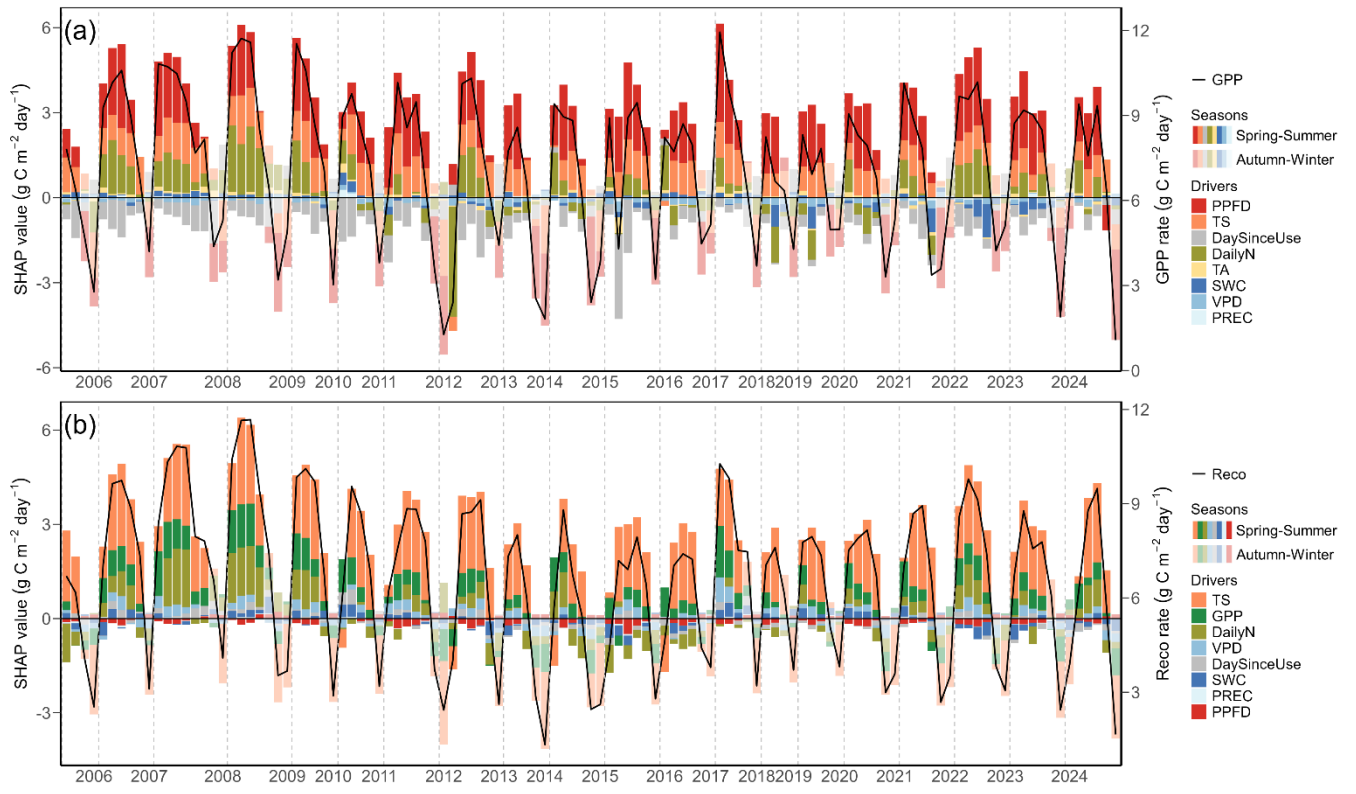


Figure 4. Drivers of (a) gross primary production (GPP) and (b) ecosystem respiration (Reco) for all regrowth periods during the years 2005 to 2024 from SHAP analysis 1.

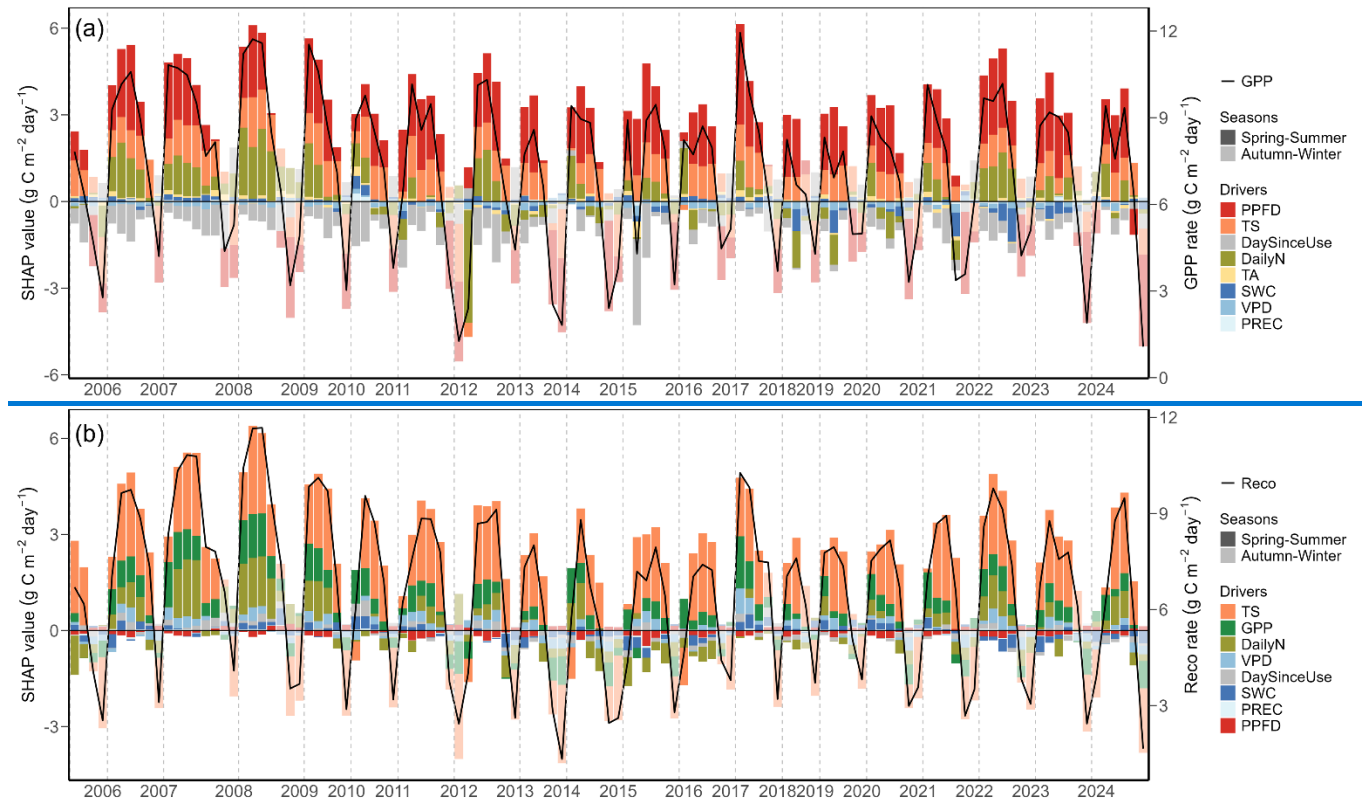


Figure 4. Drivers of (a) gross primary production (GPP) and (b) ecosystem respiration (Reco) for all regrowth periods during the years 2005 to 2024 from SHAP analysis 1. Each stacked bar represents mean SHAP values of drivers from the overall XGBoost model, presented for each regrowth period: total photosynthetic photon flux density (PPFD, red), soil temperature (TS, orange), air temperature (TA, yellow), volumetric soil water content (SWC, dark blue), vapour pressure deficit (VPD, blue), precipitation (PREC, light blue), daily fertilizer nitrogen input (DailyN, moss green), day since last mowing, grazing or renewal (DaySinceUse, grey), and gross primary production (GPP, green). The overall mean prediction for all years at SHAP value zero corresponds to a GPP of $6.1 \text{ g C m}^{-2} \text{ day}^{-1}$ and Reco of $5.3 \text{ g C m}^{-2} \text{ day}^{-1}$. Positive SHAP values represent positive impacts of drivers on GPP and Reco relative to the mean prediction, while negative values indicate negative impacts from the mean prediction. The regrowth rates of GPP and Reco during each regrowth period are shown as black lines. Bars with full opaque colours indicate regrowth periods in the spring-summer season (April-September). Bars with more transparent colours indicate regrowth periods in the autumn-winter season (October-March).

3.4 Functional relationships between PPFD and GPP

Focusing on the years with exceptional management during the 20 years of this study, i.e., the renewal years 2012 and 2021, we tested the functional relationships between PPFD and GPP for the two years before and after the renewal years vs. all other normal years (Fig. 5). During all periods, daily GPP increased with mean daily PPFD before saturating at, while maximum GPP (GPP_{max}, i.e., the maximum of the curves in Figure 5) was reached at a PPFD of about $30 \text{ mol m}^{-2} \text{ day}^{-1}$ (before the renewal for years before the renewals) or at about $45 \text{ mol m}^{-2} \text{ day}^{-1}$ (after the renewal years for all other normal

years) and years after the renewals). Moreover, spring-summer seasons in all years showed rather similar average GPP during regrowth rates periods: $8.2 \text{ g C m}^{-2} \text{ day}^{-1}$ before the renewal years, $8.6 \text{ g C m}^{-2} \text{ day}^{-1}$ after the renewal years, and $8.9 \text{ g C m}^{-2} \text{ day}^{-1}$ for normal years. However, maximum GPP (GPP_{max}, i.e. the maximum of the curves in Fig. 5) was lower before the renewal years ($8.5 \text{ g C m}^{-2} \text{ day}^{-1}$) compared to normal years ($9.7 \text{ g C m}^{-2} \text{ day}^{-1}$) and years after renewal the renewals ($9.3 \text{ g C m}^{-2} \text{ day}^{-1}$), despite the fact that both the two years (2022 and 2023) after the second renewal (2022 and 2023) experienced more frequent extreme weather conditions during summer than the normal years (Fig. 2).

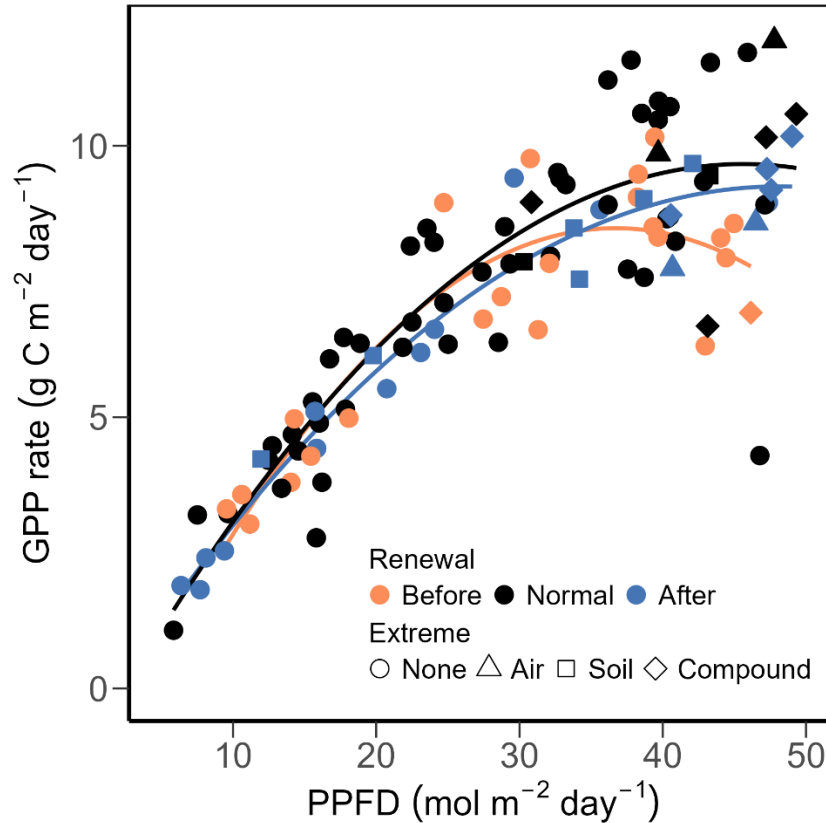
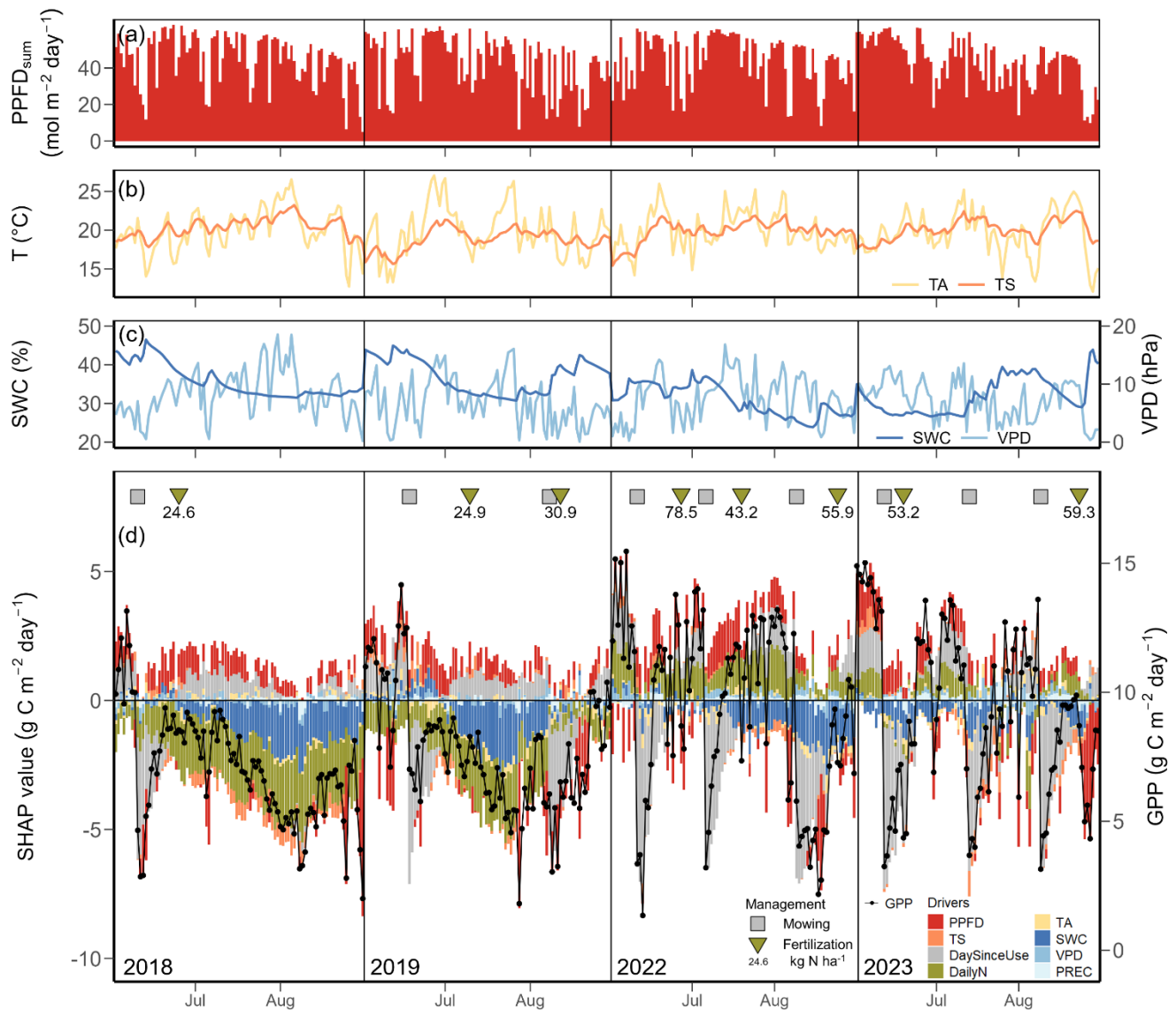


Figure 5. Relationships between mean photosynthetic photon flux density (PPFD) and regrowth rate of gross primary production (GPP) for during regrowth periods between 2005 and 2024, excluding the renewal years (2012 and 2021). Two years before the renewal years (i.e., 2010 and 2011; 2019 and 2020) are presented in orange; two years after the renewal years (2013 and 2014; 2022 and 2023) are shown in blue, while the remaining years are shown in black. Regrowth periods that spanned across extreme months (as shown in Figure Fig. 2) are shown in different shapes: high air dryness (triangles), high soil dryness (squares), and compound air and soil dryness (diamonds). Second-degree polynomial fits are shown in solid lines, with the same colour code as for the years.

375 3.5 Temporal development of GPP drivers during extreme months

Focusing on the years with extreme summer months during the peak growing season, (i.e., June, July, and August in the years of 2018, July of 2019, July of 2022, and June of 2023 (lower right hand quadrant in Fig. 2; SHAP analysis-2), we found normal daily PPFD (Fig. 6a), but significantly higher-than-normal daily temperature (TA, TS) and VPD, accompanied

by lower-than-normal ~~soil water content~~SWC (Fig. 6b-c). Mean monthly TA in July 2018, 2019, 2022 was 1.2, 1.2, and 1.1
380 °C above the 20-year monthly average (19.6 °C), respectively, and 1.8 °C higher in August 2018 compared to 20-year
monthly average (18.6 °C). All extreme summer months had SWC more than 10% lower than the 20-year monthly averages.
Daily GPP during the peak growing ~~season~~seasons (June, July, August) in 2018 and 2019 ~~was~~(i.e., years before the second
~~renewal) were~~ smaller than the mean predicted GPP of non-extreme months during the peak growing ~~season~~seasons of
normal years (9.7 g C m⁻² day⁻¹), while GPP in 2022 and 2023 ~~was~~(i.e., years after the second renewal) were more dynamic,
385 ranging from 1.3 to 15.5 g C m⁻² day⁻¹ (Fig. 6d). Mowing and fertilization events were also more frequent in the recent years
(2022, 2023) compared to earlier years (2018, 2019), accompanied by higher amounts of N input. In contrast to the findings
~~from~~over all 20 years (Fig. 4), management-related drivers, i.e., DailyN and DaySinceUse, gained higher importance during
~~these~~the extreme summer months, while PPF_D lost importance (Fig. 6d). In addition, ~~soil water content~~SWC surpassed ~~soil~~
~~temperature~~TS in importance, and its limiting ~~impac~~effect on GPP was clearly seen in all four extreme summers, stronger in
390 2018 and 2019 than in 2022 and 2023. However, ~~impac~~effects of fertilizer N inputs on GPP differed during the four
summers: In 2018 and 2019 (i.e., years before the renewal in 2021), N fertilization ~~impac~~effects acted similarly to SWC
(both drivers having negative SHAP values), suggesting low N availability during low SWC periods, while in 2022 and 2023
(i.e., years after the renewal in 2021), fertilizer N inputs increased GPP (positive SHAP values) despite low SWC values.
The relationship between SWC and its SHAP values for GPP during those four extreme summers showed a clear trend
395 ~~toward~~with limitation of GPP at low SWC (negative SHAP values; Fig. A4). This limitation of GPP by SWC was stronger in
the years 2018 and 2019 (before the renewal; lowest SHAP values) compared to the years 2022 and 2023- (after the renewal
in 2021).



400 Figure 6. Meteorological conditions and drivers of gross primary production (GPP) for days in the peak growing ~~season~~seasons (June, July, August) during the ~~extreme~~ years 2018, 2019, 2022 and 2023 from SHAP analysis 2. (a) Daily total photosynthetic photon flux density (PPFD_{sum}), (b) daily mean air temperature (TA, yellow line) and soil temperature (TS, orange line), (c) daily mean ~~volumetric~~ soil water content (SWC, dark blue line) and vapour pressure deficit (VPD, light blue line), (d) daily GPP (black dot-line) and SHAP values of each driver (stacked bar-) are given. Colours of the bars represent different drivers: photosynthetic photon flux density (PPFD, red), soil temperature (TS, orange), air temperature (TA, yellow), soil water content (SWC, dark blue), vapour pressure deficit (VPD, blue), precipitation (PREC, light blue), day since last mowing, grazing or renewal (DaySinceUse, grey), and daily fertilizer nitrogen input (DailyN, moss green). The mean prediction of GPP during non-extreme months in peak growing seasons (June, July, August) at SHAP value zero corresponds to a GPP of 9.7 g C m⁻² day⁻¹. The years 2018 and 2019 were before the grassland renewal in 2021, the years 2022 and 2023 after the grassland renewal. Positive SHAP values represent positive ~~impact~~effects of drivers on GPP relative to the mean prediction, while negative values indicate negative ~~impact~~effects from the mean prediction. Symbols in the top of panel (d) represent management events during these months: mowing (squares) and fertilization (triangles). Numbers under the triangles give the amount of total ~~fertilization~~fertilizer nitrogen (N) input. The x-axis position of each symbol indicates the date of each event.

405

410

4. Discussion

4.1 Intra- and interannual variations of CO₂ fluxes and management during 20 years

415 Overall, CO₂ fluxes (NEE, GPP, and Reco) at the Chamau grassland site showed significant intra- and inter-annual [variation](#)
([Fig. variations \(Figs. 1e, Fig. A1\)](#)), with sometimes higher inter-annual variation (-260 ± 172 , 2193 ± 263 , 1934 ± 244 g C m⁻² yr⁻¹ for NEE, GPP and Reco, respectively) than reported earlier for managed grasslands (e.g., Ammann et al., 2020; Heimsch et al., 2021, 2024; Peichl et al., 2011; Rogger et al., 2022). Reasons for these differences are manifold, considering
420 meteorological conditions and frequent management events, we also captured the impacts of multiple extreme periods,
particularly dry and hot summer months in 2018, 2019, 2022, and 2023 (Fig. 2), a six-year N₂O [mitigation](#) experiment with
reduced organic fertilization (2015 to 2020; Feigenwinter et al., 2023b), as well as infrequent management practices such as
two complete sward renewals (in 2012 and 2021; Feigenwinter et al., [in prep](#); Merbold et al., 2014), all contributing to the
highly dynamic nature of ecosystem CO₂ fluxes observed at our site.

425 With climate change, GPP of terrestrial vegetation has been observed and predicted to increase (Keenan et al., 2014; Knauer
et al., 2023; Myneni et al., 1997; Piao et al., 2007) due to CO₂ fertilization, increasing temperature, and longer growing
seasons favouring photosynthesis, unless other resources become limiting, such as water or nutrients (He et al., 2017;
Keenan et al., 2023; Madani et al., 2020; Terrer et al., 2019; Xu et al., 2019). Often, studies focused on natural [unmanaged](#)
ecosystems or forests at regional and global scales (Anav et al., 2015; Cai and Prentice, 2020; Davi et al., 2006; Norby et al.,
430 2010), but studies on grasslands also observed increasing trends in GPP and Reco with higher temperature in the past (Shi et
al., 2022; Wang et al., 2019). These studies were often based on experiments in less intensively managed or even unmanaged
grasslands, consequently with less intervention potential for farmers or land managers. In contrast, despite significant
increases in mean annual [temperatureTA](#) of around 1.4 °C over the past 20 years and decreases in [soil water contentSWC](#)
during late summer and autumn months ([Table 1 Tab. A2](#)), we did not observe significant trends in GPP nor Reco of our
435 intensively managed grassland (Fig. [33b-c](#)). This clearly indicates that despite observed climate change, the farmer managed
to maintain [GPP during regrowth ratesperiods](#) and forage production over the past two decades, also seen in the harvest
exports reported by Feigenwinter et al. (2023a) for the same site (335 ± 42 g C m⁻² yr⁻¹ between 2005 and 2020). The local
farmer adapted management practices, e.g., skipped individual harvests in extreme years (e.g., 2018), thereby extending the
regrowth periods (Fig. [A23a](#)). These detailed adjustments are typically difficult to capture by standard large-scale models
440 and coarse-resolution management datasets, demonstrating that management information at high spatio-temporal resolution
is crucial to reliably model GPP of agricultural systems. However, management data at high temporal resolution is difficult
to obtain, therefore large-scale modelling studies often use harmonized datasets at annual time scales (Winkler et al., 2021),
potentially introducing substantial bias in modelled GPP.

In addition, infrequent management events such as sward renewals, typically carried out every 5-15 years depending on
445 vegetation composition and soil texture (Schils et al., 2007; SUPER-G, 2018), are typically not considered in C cycle

models, partially due to lack of information about their occurrence but also simply due to lack of data for such events. ~~For our site, two renewal events in 2012 and 2021 were included in the long time series (Fig. 1e, A1), with very different effects on NEE: while the event in 2012 led to a strong net CO₂ loss (cumulative NEE of 139 g C m⁻² yr⁻¹; Fig. 1e, A1), the event in 2021 resulted only in a weaker than normal net CO₂ uptake (cumulative NEE of -163 g C m⁻² yr⁻¹; Fig. A1). The two renewal events differed~~ in seasons (February 2012 versus August 2021) and soil disturbance intensities (ploughed at 20 cm in 2012 and 3-4 cm in 2021), which subsequently influenced the establishment and regrowth of the new sward, ~~likely explaining the observed difference in NEE.~~ Other studies in managed grasslands have also reported different magnitudes of CO₂ fluxes after renewal, influenced by timing, intensity, and environmental conditions of the renewal events (Ammann et al., 2020; Drewer et al., 2017; Li et al., 2023b). Such observations, albeit rare, ~~but are~~ impactful in terms of C dynamics, ~~and~~ underscore the necessity to include such infrequent destructive management practices in long-term flux studies as well as modelling frameworks.

4.2 Temporal development of driver contributions during regrowth periods using machine learning

NEE represents a combination of two large opposing fluxes, i.e., GPP and Reco, based on two physiological processes, i.e., photosynthesis and respiration, which respond differently to changing environmental conditions (Feigenwinter et al., 2023a; Peichl et al., 2011; Schwalm et al., 2010; Wang et al., 2019). Thus, using two separate machine learning models for GPP and Reco (XGBoost models with high performance, $R^2 > 0.9$ on testing datasets), we identified ~~the their~~ main ~~GPP and Reco~~ drivers as well as the temporal development of daily driver contributions (SHAP analysis 1). ~~Confounding effects from overlapping predictor variables were reduced by using a broader set of variables for the driver analysis compared to the gap-filling model. Daily aggregated data for the driver analysis (instead of half hourly as for gap-filling) furthermore reduced potential correlation among predictor variables.~~ In contrast to other studies, we not only included high resolution meteorological data but also information about management events in our analyses at daily time scales. Consistent with previous studies (Gilmanov et al., 2007; Wohlfahrt et al., 2008), PPFD and temperature were the main drivers of GPP and Reco, respectively (Fig. 4, A3A2). However, management-related variables such as the number of days since the last management event and fertilizer N inputs were always among the top four to five important drivers for daily GPP and Reco, respectively, ~~highlighting. This highlights~~ their importance for a ~~mechanistic comprehensive~~ understanding of C dynamics and greenhouse gas fluxes in managed grasslands (Hörtnagl et al., 2018-2018). ~~By using time since the last management event (i.e., DaySinceUse) as a driver, we incorporated the management information into the models in a relatively straightforward way. This variable enabled the models to capture the management-related patterns in GPP and Reco that could not be explained by other meteorological variables. However, the simplification of our approach should also be recognised: DaySinceUse is not an ecophysiological driver, instead, it functions as a proxy for otherwise neglected management events.~~ The machine learning analyses also picked up the smaller effects of fertilizer N inputs as a driver for GPP during the N₂O mitigation experiment (2015 to 2020), when organic fertilization – and thus N inputs – was replaced

with higher fractions of legumes for half of the area (Feigenwinter et al., 2023b; Fuchs et al., 2018). Since the majority of
480 temperate grasslands in Europe are actively managed (Eurostat, 2023), long-term and detailed management information,
combined with more field observational measurements such as EC fluxes, can support improved management strategies to
enhance grassland ecosystem services under changing climate (Wang et al., 2025b). [Although detailed management
information has been used successfully in our XGBoost models, we also acknowledge the limitation from our simplified
representation of N fertilization on the daily scale. We represented N availability after fertilization by distributing the total N
485 applied evenly across the regrowth period \(see Section 2.2\), although the actual temporal dynamics of N availability most
likely follow a more complex pattern, involving different processes and drivers such as soil properties, precipitation, soil
moisture and temperature but also microbial activity. However, such data are very rare, and model assumptions can thus
often not be validated due to insufficient evidence in the existing literature. While we employed a simplified approach, we
clearly recognize the need for remotely sensed or *in-situ* quantified daily N availability to further improve modelling of CO₂
490 fluxes in managed grasslands.](#)

Focusing on GPP and its most important driver PPFD, we further examined the physiological consequences of the two
renewals in 2012 and 2021. Although the sward had shown a lower performance before the renewals, (i.e., lower GPPmax, ~~orange line~~,
orange line, Fig. 5), compared to the following years with higher GPPmax (black and blue lines), the slopes of the light-
response curves were very similar. Differences in GPPmax resulted in high net CO₂ uptake rates after both renewals (average
495 cumulative NEE of -465 g C m⁻² yr⁻¹ for 2013, 2014, 2022, and 2023) and also higher yields than before the renewals ([Table
A3, Tabs. A4, A5](#)). Thus, the farmer's decision to renew the grassland with a multi-species mixture was substantiated.
Furthermore, frequent oversowing ([Table Tables B1 and B2](#) in Feigenwinter et al., 2023a) might further help to maintain the
preferred species composition and a stable yield. However, even though oversowing more diverse mixtures (Schaub et al.,
2020) or increasing ~~the~~ legume proportions (Fuchs et al., 2018) can ~~also improve the~~ yield quality and are less destructive
500 management interventions than sward renewals, they can be costly (Schaub et al., 2021), and positive results are not always
guaranteed. Therefore, adopting a combination of these observed management practices is a crucial first step towards more
climate-smart farming [practices](#), helping to ensure stable production and [to](#) sustain ecosystem services over the long
term.

Besides consistent positive effects of light and temperature on GPP (Fig. 4; red and orange bars), fertilizer N inputs ([Fig. 4;](#)
505 moss green bars) also promoted GPP during spring-summer seasons. Moreover, our analysis demonstrated the complex
interactions between N inputs and soil water availability: the positive [impacts](#) of N on GPP diminished in drier years
(e.g., 2018, 2019) or even became negative, indicating lower soil N availability and thus lower N uptake for GPP when soil
moisture was low (Bloor and Bardgett, 2012; Hartmann et al., 2013). For Reco, negative effects of N inputs were more
obvious during the spring-summer seasons 2015 to 2020, i.e., when the N₂O mitigation experiment was ongoing, and the
510 entire site received around half of fertilizer N input compared to other years (Feigenwinter et al., 2023b; Fuchs et al., 2018).
Without N inputs via organic fertilizer (mostly slurry), the organic C inputs and the C sink strength were reduced as well
(Feigenwinter et al., 2023a). This resulted in less C available for microbial soil respiration, which was also reflected [by](#)

lower Reco during regrowth rates periods in spring-summer seasons during the N₂O mitigation experiment ($7.4 \pm 1.3 \text{ g C m}^{-2} \text{ day}^{-1}$) ~~than~~ compared to Reco in years with normal management ($8.2 \pm 1.7 \text{ g C m}^{-2} \text{ day}^{-1}$).

515 Overall, being purely data-driven and highly site-dependent, the combination of machine learning models and SHAP analysis confirmed the highly dynamic nature of the drivers influencing GPP and Reco and also revealed the complexity of their individual contributions across temporal scales. Compared to traditional linear models, these new approaches not only captured the non-linear and combined effects among drivers at high temporal resolution (here daily), but also provided explanatory outputs such as driver importance on a daily basis, which enhanced interpretability of the machine learning
520 models and further improved our understanding of these complex grassland systems.

4.3 Drivers during extreme growing seasons

Using non-extreme summer months as the background dataset, SHAP analysis 2 focused on drivers of GPP only during extreme summer months, which minimized the confounding effects of strong seasonality in temperature and light conditions. This approach further improved the interpretability of our results, by isolating and focusing on the influence of extreme events-related factors such as SWC and VPD. Across all extreme periods, SWC strongly reduced GPP (SHAP analysis 2; Fig. 6d). In contrast, the impacted effect of VPD was small (Fig. 6d), even on days with exceptionally high VPD values (Fig. 6c). This finding supported our long-term driver analysis (SHAP analysis 1; Fig. 4), ~~where~~: here, SWC had a larger impacted effect on GPP than VPD (mean absolute SHAP value of 0.6 for SWC and 0.2 for VPD during the peak growing seasons in 2018, 2019, 2022, and 2023), underscoring that soil water availability was more relevant for GPP than
530 atmospheric water demand. This observation aligns well with previous studies reporting more significant negative effects of soil droughts (i.e., low SWC) on grassland CO₂ fluxes compared to those of heatwaves (i.e., high VPD; Li et al., 2016, 2021). ~~Our finding~~ is also consistent with the behaviour seen during the 2003 summer drought (Teuling et al., 2010) and the 2018 summer drought (Gharun et al., 2020), during which grasslands sustained evapotranspiration (ET) and thus GPP, as long as water was available in the soil, much in contrast to forests which rapidly reduced stomatal canopy conductance and
535 ET in response to high VPD.

The effects of fertilizer N inputs were more differentiated during these extreme periods compared to the overall 20-year time series. While N inputs showed mostly negative impacted effects on GPP during the years 2018 and 2019 (i.e., during the N₂O mitigation experiment and before the second renewal in 2021), effects of N inputs were typically positive during the years 2022 and 2023 (Fig. 6d). This suggests that after the second sward renewal in 2021, a resumed organic fertilization regime
540 with a higher amount of fertilizer N input could further help the support recovery and increase regrowth rates after extreme periods (Hofer et al., ~~2016~~2017). Additionally, in response to the persistent droughts in 2018 and 2019 before the second renewal, the farmer delayed or skipped some mowing events (which typically occurred monthly during the peak growing season, ~~Fig~~Figs. 6d ~~and A2~~, 3a). In contrast, we observed even more frequent mowing events (three times between June and August) during 2022 and 2023 after the second renewal, which resulted in more regrowth periods and more variation in GPP
545 compared to earlier years. ~~This indicates~~ While the first renewal in 2012 also resulted in increased productivity and forage

yields (Feigenwinter et al., 2023a), our study clearly indicated that also after the second renewal in 2021 the new sward performed very well despite the frequent and more intense extreme conditions in these two succeeding years compared to earlier years, the new grassland sward performed well and sustained the sustaining forage production also during such extreme summers.

550 Over the past two decades, Switzerland has experienced its hottest years on record (2022, 2023) and several extreme summers (e.g., 2018, 2022) (MeteoSwiss, 2023, 2024; Scherrer et al., 2022). In our study, we also observed consistent trends of rising temperature and frequent extreme summer months in recent years. The CO₂ fluxes of this intensively managed grassland responded highly very dynamically to changes in meteorology and to the already climate-adjusted management practices implemented by the farmer. However, it is unclear whether such small adjustments will suffice when extreme

555 events intensify in the future (CH2018, 2018CH2025; IPCC, 2023). Although some Some evidence suggested that less intensive management may buffer grasslands against extreme impact (Winck et al., 2025), adopting a less intensive management scheme—which would require a different sward composition, lower livestock density, and further adjusted management practices—is challenging. Adopting a less intensive management scheme for a single grassland site in a short time period is challenging. Therefore, site-specific adaptation of management strategies for both short- and long-term

560 is needed to mitigate current and future climate risks (Gilgen and Buchmann, 2009; Woo et al., 2022). Further management options, such as multi-species mixtures (Craven et al., 2016; Finn et al., 2018; Isbell et al., 2015; Wang et al., 2025b) and spatially adjusted precision-farming (Finger et al., 2019), can offer additional highly site-specific solutions to maintain selected ecosystem services and support the resilience of grasslands against extreme events.

5. Conclusions

565 Using a long-term dataset of CO₂ fluxes and detailed management information, our study provided unique and novel insights into temporal dynamics of CO₂ fluxes and their drivers. With state-of-the-art machine learning tools, we were able to identify and attribute the effects of different drivers, i.e., management and meteorological conditions, and their complex temporal dynamics, which would have been impossible with classical statistical approaches. While management-related drivers showed high importance for grassland CO₂ fluxes, such information is unfortunately often lacking, creating large

570 uncertainties in C cycle models model simulations at all scales. Therefore, we call for reliable collection and sharing of management data according to FAIR (Findable, Accessible, Interoperable, and Reusable) principles, alongside the highly valuable long-term observational data. Open science strongly improves our understanding of these highly dynamic grassland systems and enables development of realistic solutions under future climate conditions. Moreover, during the based on two decades of our measurements, our evidence suggests that the grassland farmers farmer succeeded in managing the site with

575 relatively stable GPP during regrowth rates through periods, based on climate-smart adaptive management and interventions, already demonstrating effective climate smart strategies. With increasing climate risks, additional practices like multi-

species mixtures and [spatially adjusted management practices such as](#) precision-farming, but also early warning systems for extreme events will become crucial to further enhance the resilience of grassland-based farming systems in the future.

Table A1. The best hyperparameters used in the XGBoost models for GPP and Reco

Hyperparameters	GPP	Reco
n_estimators	2000	2000
max_depth	5	5
learning_rate	0.05	0.1
subsample	0.8	1
colsample_bytree	1	1
min_child_weight	10	10
reg_lambda	10	10

Table A2. Monthly meteorological variables from 2005 to 2024. For each month, mean and standard deviation (SD), trends (unit yr⁻¹; in non-italics positive trends, in italics negative trends) and significance from Mann-Kendall test (p-values < 0.05: *, < 0.01: **) are shown.

Variable	Unit	Jan		Feb		Mar		Apr	
		Mean±SD	Trend	Mean±SD	Trend	Mean±SD	Trend	Mean±SD	Trend
TA_mean	°C	<u>0.96±1.95</u>		<u>1.84±2.41</u>	<u>0.2*</u>	<u>5.26±1.3</u>		<u>9.48±1.36</u>	
TA_min	°C	<u>-10.22±3.58</u>		<u>-8.96±3.74</u>		<u>-6.48±3.03</u>	<u>0.253*</u>	<u>-3.05±1.56</u>	
TA_max	°C	<u>12.45±3.36</u>		<u>15.01±3.48</u>		<u>19.8±2.26</u>		<u>24.35±2.33</u>	
TS_mean	°C	<u>3.9±1.23</u>	<u>0.144**</u>	<u>3.79±1.48</u>	<u>0.164**</u>	<u>6.16±1.18</u>	<u>0.121*</u>	<u>10.07±0.73</u>	
TS_min	°C	<u>2.24±1.05</u>	<u>0.096**</u>	<u>1.97±1.14</u>	<u>0.11**</u>	<u>3.43±1.47</u>	<u>0.141*</u>	<u>6.49±1.27</u>	
TS_max	°C	<u>6.15±1.56</u>	<u>0.162*</u>	<u>6.33±1.57</u>	<u>0.162*</u>	<u>9.81±1.34</u>		<u>13.84±1.54</u>	
PREC_sum	mm	<u>64.28±35.59</u>		<u>48.81±23.57</u>		<u>65.68±34.35</u>		<u>83.51±48.92</u>	
SWC_mean	%	<u>48.19±2.19</u>		<u>48.07±2.16</u>		<u>47.65±2.99</u>	<u>-0.236*</u>	<u>45.15±3.85</u>	
SWC_min	%	<u>46.21±2.49</u>		<u>46.3±2.94</u>		<u>45.39±3.51</u>	<u>-0.302*</u>	<u>41.08±4.96</u>	
SWC_max	%	<u>49.76±2.19</u>		<u>49.57±2.25</u>		<u>49.07±2.47</u>		<u>46.77±4.01</u>	
VPD_mean	hPa	<u>0.73±0.36</u>		<u>1.2±0.39</u>		<u>2.36±0.61</u>		<u>3.8±1.17</u>	
VPD_max	hPa	<u>6.55±2.02</u>	=	<u>10.13±3.51</u>	=	<u>15.6±3.16</u>	=	<u>21.28±4.9</u>	=

Table A2. (continued)

Variable	May		Jun		July		Aug	
	Mean±SD	Trend	Mean±SD	Trend	Mean±SD	Trend	Mean±SD	Trend
TA_mean	<u>13.77±1.51</u>		<u>18.1±1.11</u>		<u>19.55±1.35</u>		<u>18.61±1.45</u>	<u>0.157**</u>
TA_min	<u>1.47±2.08</u>		<u>5.9±1.64</u>		<u>8.41±1.37</u>		<u>7.56±1.09</u>	
TA_max	<u>28.18±2.56</u>		<u>32.28±1.93</u>		<u>33.71±1.7</u>		<u>32.42±2.63</u>	
TS_mean	<u>13.83±1.06</u>		<u>17.91±1.07</u>		<u>20.08±1.15</u>		<u>19.62±1.04</u>	<u>0.092*</u>
TS_min	<u>10.58±1.14</u>		<u>14.02±1.39</u>		<u>17.1±0.8</u>		<u>16.85±1</u>	

<u>TS_max</u>	<u>17.73±1.83</u>		<u>22.1±1.99</u>		<u>23.5±1.92</u>		<u>22.91±1.67</u>	
<u>PREC_sum</u>	<u>135.84±49.35</u>		<u>140.56±52.47</u>		<u>148.2±71.1</u>		<u>142.83±46.43</u>	<u>-4.057*</u>
<u>SWC_mean</u>	<u>44.46±3.89</u>		<u>42.78±5.34</u>		<u>42.17±5.83</u>		<u>41.74±5.69</u>	<u>-0.468*</u>
<u>SWC_min</u>	<u>39.28±4.92</u>		<u>38.13±5.85</u>	<u>-0.356*</u>	<u>37.16±5.45</u>		<u>37.25±5.69</u>	
<u>SWC_max</u>	<u>45.94±3.97</u>		<u>44.66±5.25</u>		<u>44.34±5.37</u>		<u>44.29±5.02</u>	
<u>VPD_mean</u>	<u>4.5±1.26</u>		<u>6.21±1.41</u>		<u>6.9±1.69</u>		<u>5.43±1.4</u>	
<u>VPD_max</u>	<u>25.57±4.74</u>	=	<u>32.02±4.52</u>	=	<u>35.82±6.37</u>	=	<u>29.97±7.05</u>	=

Table A2. (continued)

<u>Variable</u>	<u>Sep</u>		<u>Oct</u>		<u>Nov</u>		<u>Dec</u>	
	<u>Mean±SD</u>	<u>Trend</u>	<u>Mean±SD</u>	<u>Trend</u>	<u>Mean±SD</u>	<u>Trend</u>	<u>Mean±SD</u>	<u>Trend</u>
<u>TA_mean</u>	<u>14.91±1.4</u>		<u>10.36±1.32</u>		<u>5.01±1.06</u>		<u>1.54±1.44</u>	
<u>TA_min</u>	<u>3.72±1.65</u>		<u>0.26±2.49</u>		<u>-4.75±3.01</u>	<u>0.252*</u>	<u>-8.73±3.91</u>	
<u>TA_max</u>	<u>28.4±1.76</u>		<u>23.56±2.28</u>		<u>16.96±2.84</u>		<u>12.41±1.98</u>	
<u>TS_mean</u>	<u>16.96±1.03</u>		<u>13.41±0.81</u>		<u>9.02±1.12</u>	<u>0.102*</u>	<u>5.41±1.24</u>	<u>0.123**</u>
<u>TS_min</u>	<u>13.91±1.17</u>		<u>10.46±1.57</u>	<u>0.128*</u>	<u>6±1.79</u>	<u>0.18*</u>	<u>3.69±1.2</u>	<u>0.174**</u>
<u>TS_max</u>	<u>20.35±1.79</u>		<u>16.46±1.05</u>		<u>12.1±1.2</u>		<u>7.54±1.36</u>	<u>0.119*</u>
<u>PREC_sum</u>	<u>93.18±44.69</u>		<u>76.67±28.61</u>		<u>66.45±44.14</u>		<u>81.25±44.07</u>	
<u>SWC_mean</u>	<u>42.43±5.16</u>	<u>-0.44*</u>	<u>43.79±4.26</u>	<u>-0.399*</u>	<u>45.74±3.34</u>		<u>47.72±3.05</u>	
<u>SWC_min</u>	<u>38.64±5.09</u>	<u>-0.538*</u>	<u>40.98±4.64</u>		<u>43.62±3.41</u>		<u>45.86±3.07</u>	
<u>SWC_max</u>	<u>44.85±4.57</u>	<u>-0.351*</u>	<u>46.01±3.8</u>	<u>-0.306*</u>	<u>47.33±3.31</u>		<u>49.24±3.02</u>	
<u>VPD_mean</u>	<u>3.28±0.65</u>		<u>1.54±0.52</u>		<u>0.76±0.37</u>	<u>-0.032*</u>	<u>0.53±0.34</u>	
<u>VPD_max</u>	<u>21.64±3.8</u>	=	<u>14.92±4.08</u>	=	<u>8.48±2.87</u>	=	<u>5.51±1.27</u>	=

590

Table A3. GPP and Reco from 2005 to 2024 under three different scenarios: for the 16th (U_16), 50th (U_50), and 84th (U_84) percentile of the USTAR threshold distribution respectively.

<u>Year</u>	<u>GPP_U50</u>	<u>Reco_U50</u>	<u>GPP_U16</u>	<u>GPP_U50</u>	<u>GPP_U84</u>	<u>Reco_U16</u>	<u>Reco_U50</u>	<u>Reco_U84</u>
	<u>Annual sum (g C m⁻² yr⁻¹)</u>		<u>Mean and standard deviation of daily sum (g C m⁻² day⁻¹)</u>					
2005	1929	1646	5.1 ± 3.7	5.3 ± 4.0	5.7 ± 4.3	4.3 ± 2.0	4.5 ± 2.2	5.1 ± 3.0
2006	2059	1934	5.6 ± 4.2	5.6 ± 4.3	6.0 ± 4.4	5.1 ± 3.2	5.3 ± 3.3	5.4 ± 3.5
2007	2506	2270	6.9 ± 4.1	6.9 ± 4.0	7.2 ± 4.3	6.2 ± 3.5	6.2 ± 3.6	6.4 ± 3.8
2008	2764	2618	7.3 ± 4.5	7.6 ± 4.7	7.6 ± 4.6	6.6 ± 3.3	7.2 ± 3.6	7.0 ± 3.5
2009	2487	2200	6.9 ± 4.5	6.8 ± 4.3	7.1 ± 4.5	6.2 ± 3.4	6.0 ± 3.0	6.4 ± 3.3
2010	2055	1908	5.4 ± 3.5	5.6 ± 3.6	5.5 ± 3.6	4.9 ± 2.7	5.2 ± 2.9	5.0 ± 2.6
2011	2164	2004	5.7 ± 3.4	5.9 ± 3.5	6.1 ± 3.7	5.1 ± 2.4	5.5 ± 2.7	5.6 ± 2.8
2012	1483	1621	4.0 ± 3.7	4.1 ± 3.7	4.2 ± 3.8	4.3 ± 2.6	4.4 ± 2.7	4.5 ± 2.8
2013	2036	1569	5.4 ± 3.8	5.6 ± 3.8	6.0 ± 4.2	4.2 ± 2.5	4.3 ± 2.6	5.0 ± 3.1
2014	2262	1759	6.3 ± 4.0	6.2 ± 3.9	6.7 ± 4.3	5.1 ± 2.6	4.8 ± 2.5	5.5 ± 2.9

2015	2112	1637	5.7 ± 3.5	5.8 ± 3.5	6.4 ± 3.8	4.4 ± 2.4	4.5 ± 2.5	5.4 ± 2.7
2016	2263	1781	6.1 ± 3.6	6.2 ± 3.6	6.6 ± 3.9	4.7 ± 2.2	4.9 ± 2.3	5.2 ± 2.5
2017	2429	2176	6.6 ± 4.3	6.7 ± 4.3	6.9 ± 4.4	5.8 ± 3.3	6.0 ± 3.3	6.1 ± 3.5
2018	1944	1898	5.2 ± 2.9	5.3 ± 3.0	5.8 ± 3.4	5.0 ± 2.2	5.2 ± 2.3	5.7 ± 2.8
2019	2123	2001	5.7 ± 3.1	5.8 ± 3.2	6.2 ± 3.4	5.3 ± 2.4	5.5 ± 2.5	5.9 ± 2.9
2020	2217	1969	6.0 ± 3.3	6.1 ± 3.3	6.4 ± 3.5	5.3 ± 2.3	5.4 ± 2.4	5.7 ± 2.6
2021	2061	1897	5.5 ± 3.8	5.6 ± 3.9	5.9 ± 4.1	5.0 ± 2.5	5.2 ± 2.7	5.4 ± 2.9
2022	2451	1970	6.8 ± 4.1	6.7 ± 4.0	7.3 ± 4.4	5.6 ± 2.8	5.4 ± 2.8	6.1 ± 3.0
2023	2274	1865	6.1 ± 4.1	6.2 ± 4.1	6.6 ± 4.4	4.9 ± 2.7	5.1 ± 2.7	5.5 ± 3.1
2024	2248	1950	6.1 ± 4.0	6.1 ± 3.9	6.4 ± 4.2	5.3 ± 2.8	5.3 ± 2.7	5.7 ± 2.8

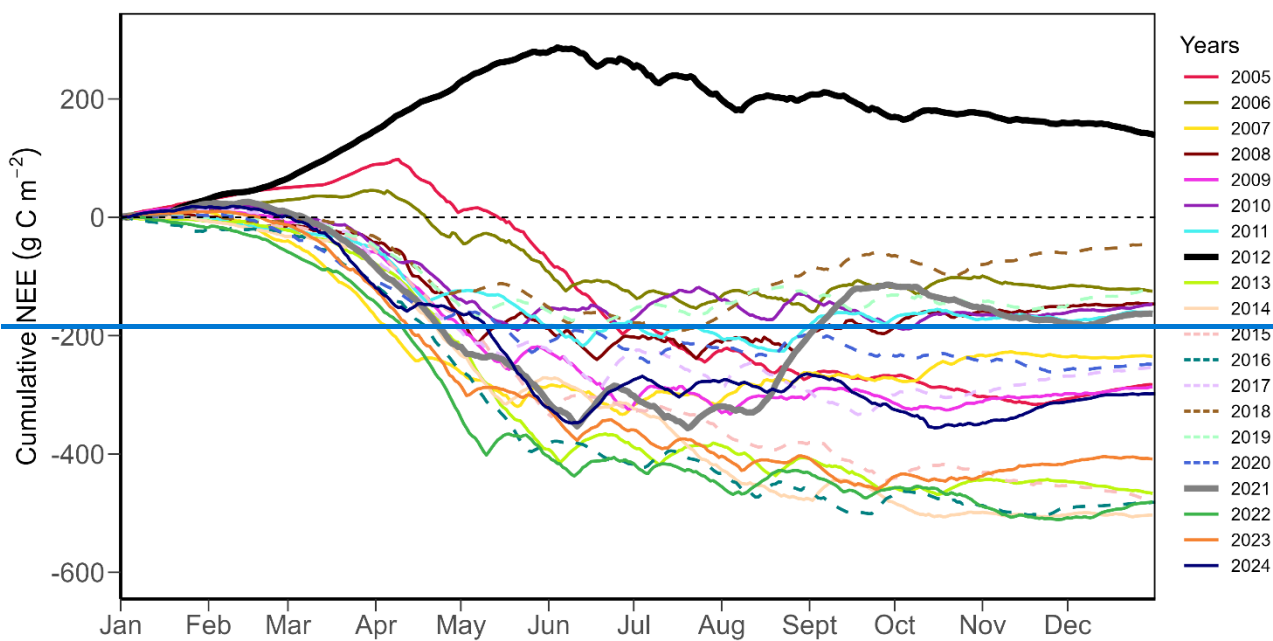
595 | **Table A3A4.** Management events per parcel from 2021 to 2024, [continuingexpanding](#) Table B1 in Feigenwinter et al. (2023a). The number of each management activity in each year is indicated in round brackets. For grazing, the duration in days is given. Fertilizer N and C [import,imports](#) as well as total yields (from mowing and grazing) are given. Years [wherewith](#) missing yield data are indicated (* yield from one mowing event missing; ** yield from one grazing event missing).

Year	Parcel	Management	Fertilizer N import (kg N ha ⁻¹)	Fertilizer C import (kg C ha ⁻¹)	Yield (kg DM ha ⁻¹)
2021	A	Mowing (4), Grazing (6 d), Fertilization (4), Herbicide (1), Tillage (1), Resowing (2)	237	1012	10127
2021	B	Mowing (4), Grazing (6 d), Fertilization (4), Herbicide (1), Tillage (1), Resowing (1)	198	795	9010
2022	A	Mowing (5), Grazing (5 d), Fertilization (6)	396	2384	13253*
2022	B	Mowing (5), Grazing (5 d), Fertilization (6)	396	2384	13613*
2023	A	Mowing (6), Fertilization (5), Herbicide (1)	291	1548	14065
2023	B	Mowing (6), Fertilization (5), Herbicide (1)	291	1548	13679
2024	A	Mowing (4), Grazing (16 d), Fertilization (5), Herbicide (1), Harrowing (1), Rolling (1)	314	1928	12527**
2024	B	Mowing (4), Grazing (16 d), Fertilization (5), Herbicide (1), Harrowing (1), Rolling (1)	314	1928	12571**

600 Table A4A5: Detailed information about management events from 2021 to 2024, [continuingexpanding](#) Table B2 in Feigenwinter et al. (2023a). The amount of harvested yield (kg DM ha⁻¹), fertilizer applied (m³ ha⁻¹), number of animals (number ha⁻¹) and duration (days) for grazing, as well as fertilizer N and C [import/imports](#) (kg C or N ha⁻¹) are reported.

Date	Parcel	Management	Amount (ha ⁻¹)/Duration	Fertilizer C (kg C ha ⁻¹)	Fertilizer N (kg N ha ⁻¹)
2021-02-23	A, B	Organic fertilizer	60 m ³ ha ⁻¹ A, 40 m ³ ha ⁻¹ B	652 A, 435 B	116 A, 77 B
2021-05-03	A, B	Mowing	3712 kg DM ha ⁻¹ A, 2452 kg DM ha ⁻¹ B		
2021-05-07	A, B	Organic fertilizer	43 m ³ ha ⁻¹	138	50
2021-06-12	A, B	Mowing	2842 kg DM ha ⁻¹ A, 2817 kg DM ha ⁻¹ B		
2021-06-18	A, B	Organic fertilizer	28 m ³ ha ⁻¹	107	53
2021-07-21	A, B	Mowing	1919 kg DM ha ⁻¹ A, 2548 kg DM ha ⁻¹ B		
2021-07-29	A, B	Organic fertilizer	28 m ³ ha ⁻¹	115	18
2021-08-13	A, B	Herbicide			
2021-08-20	A, B	Tillage (3-4 cm)			
2021-08-20	A, B	Resowing	35 kg ha ⁻¹		
2021-09-09	A	Resowing	35 kg ha ⁻¹		
2021-10-14	A, B	Mowing	1126 kg DM ha ⁻¹ A, 681 kg DM ha ⁻¹ B		
2021-12-09	A, B	Grazing	529 kg DM ha ⁻¹ A, 513 kg DM ha ⁻¹ B, 36 Animals ha ⁻¹ , 6 days		
2022-03-14	A, B	Organic fertilizer	31 m ³ ha ⁻¹	516	83
2022-05-10	A, B	Mowing	5265 kg DM ha ⁻¹ A, 5051 kg DM ha ⁻¹ B		
2022-05-23	A, B	Organic fertilizer	26 m ³ ha ⁻¹	279	57
2022-06-10	A, B	Mowing	Yield data not available.		
2022-06-27	A, B	Organic fertilizer	33 m ³ ha ⁻¹	542	78
2022-07-06	A, B	Mowing	2185 kg DM ha ⁻¹ A, 2176 kg DM ha ⁻¹ B		
2022-07-20	A, B	Organic fertilizer	29 m ³ ha ⁻¹	238	43
2022-08-09	A, B	Mowing	3160 kg DM ha ⁻¹ A, 3322 kg DM ha ⁻¹ B		
2022-08-25	A, B	Organic fertilizer	28 m ³ ha ⁻¹	293	56
2022-09-21	A, B	Mowing	1672 kg DM ha ⁻¹ A, 1867 kg DM ha ⁻¹ B		
2022-10-05	A, B	Organic fertilizer	43 m ³ ha ⁻¹	515	79
2022-12-11	A, B	Grazing	972 kg DM ha ⁻¹ A, 1196 kg DM ha ⁻¹ B, 45 Animals ha ⁻¹ , 5 days		
2023-03-21	A, B	Organic fertilizer	33 m ³ ha ⁻¹	261	60
2023-03-30	A, B	Herbicide			
2023-05-04	A, B	Mowing	3935 kg DM ha ⁻¹ A, 4798 kg DM ha ⁻¹ B		
2023-05-25	A, B	Organic fertilizer	26 m ³ ha ⁻¹	356	64
2023-06-11	A, B	Mowing	2627 kg DM ha ⁻¹ A, 2559 kg DM ha ⁻¹ B		
2023-06-19	A, B	Organic fertilizer	23 m ³ ha ⁻¹	288	53
2023-07-13	A, B	Mowing	2169 kg DM ha ⁻¹ A, 1729 kg DM ha ⁻¹ B		
2023-08-09	A, B	Mowing	1536 kg DM ha ⁻¹ A, 1551 kg DM ha ⁻¹ B		
2023-08-24	A, B	Organic fertilizer	24 m ³ ha ⁻¹	340	59
2023-09-25	A, B	Mowing	2812 kg DM ha ⁻¹ A, 2282 kg DM ha ⁻¹ B		
2023-09-29	A, B	Organic fertilizer	24 m ³ ha ⁻¹	302	55
2023-10-28	A, B	Mowing	985 kg DM ha ⁻¹ A, 760 kg DM ha ⁻¹ B		

2024-01-20	A, B	Grazing	Yield data not available. 33 Animals ha ⁻¹ , 4 days		
2024-02-28	A, B	Organic fertilizer	29 m ³ ha ⁻¹	440	61
2024-03-19	A	Herbicide			
2024-03-22	B	Herbicide			
2024-04-11	A, B	Mowing	2387 kg DM ha ⁻¹ A, 2914 kg DM ha ⁻¹ B		
2024-05-02	A, B	Organic fertilizer	23 m ³ ha ⁻¹	253	52
2024-06-11	A, B	Mowing	4119 kg DM ha ⁻¹ A, 3827 kg DM ha ⁻¹ B		
2024-06-20	A, B	Harrowing			
2024-06-20	A, B	Rolling			
2024-06-27	A, B	Organic fertilizer	30 m ³ ha ⁻¹	454	67
2024-07-17	A, B	Mowing	2667 kg DM ha ⁻¹ A, 2942 kg DM ha ⁻¹ B		
2024-08-07	A, B	Organic fertilizer	25 m ³ ha ⁻¹	370	59
2024-08-22	A, B	Mowing	1868 kg DM ha ⁻¹ A, 1359 kg DM ha ⁻¹ B		
2024-08-27	A, B	Organic fertilizer	31 m ³ ha ⁻¹	412	75
2024-11-08	A, B	Grazing	1487 kg DM ha ⁻¹ A, 1529 kg DM ha ⁻¹ B, 65 Animals ha ⁻¹ , 12 days		



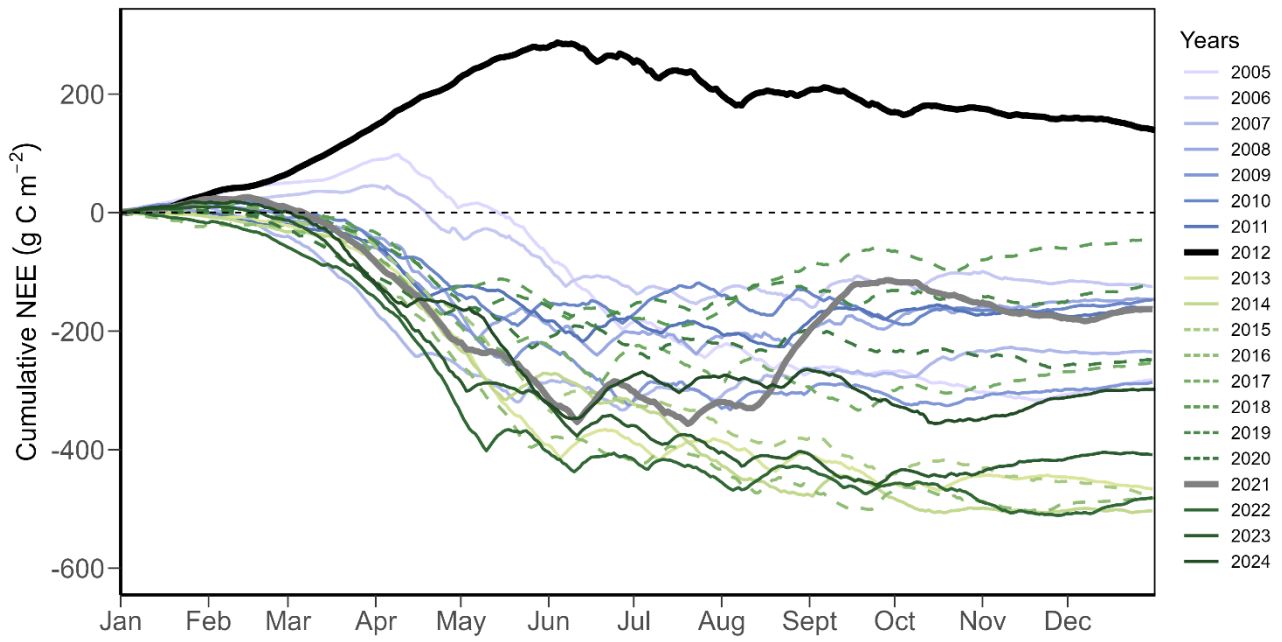
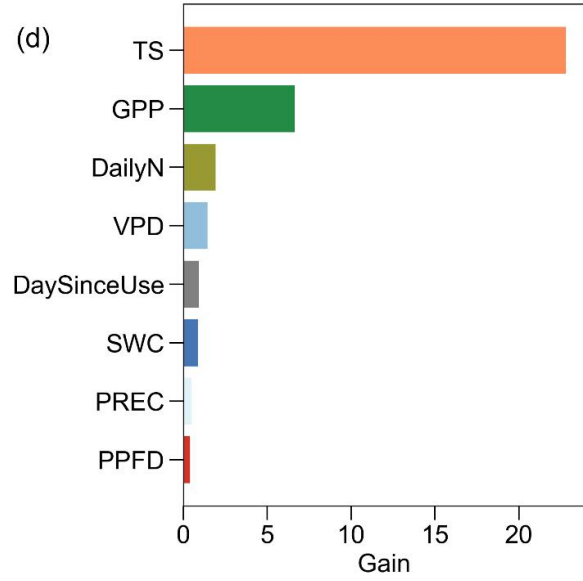
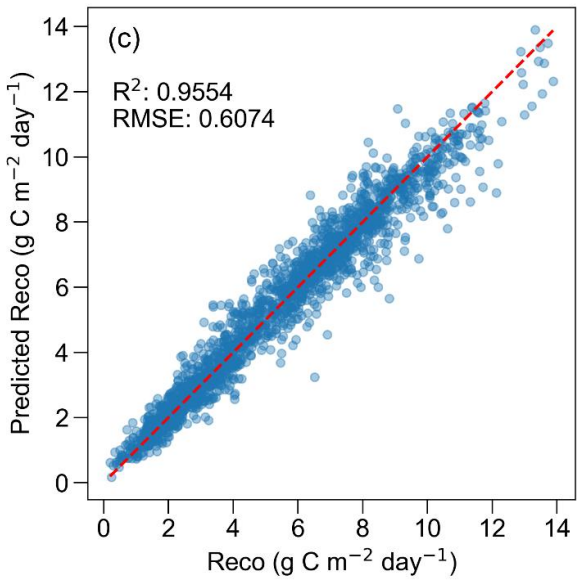
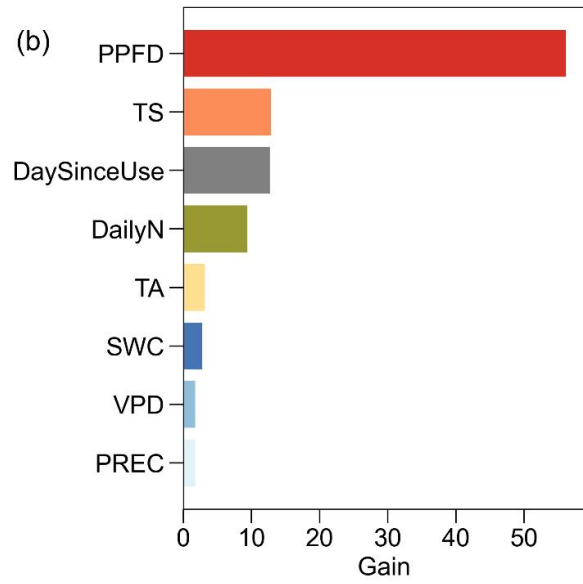
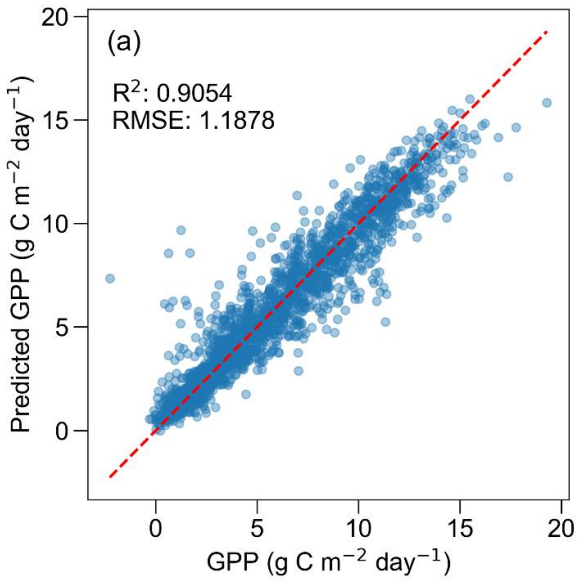
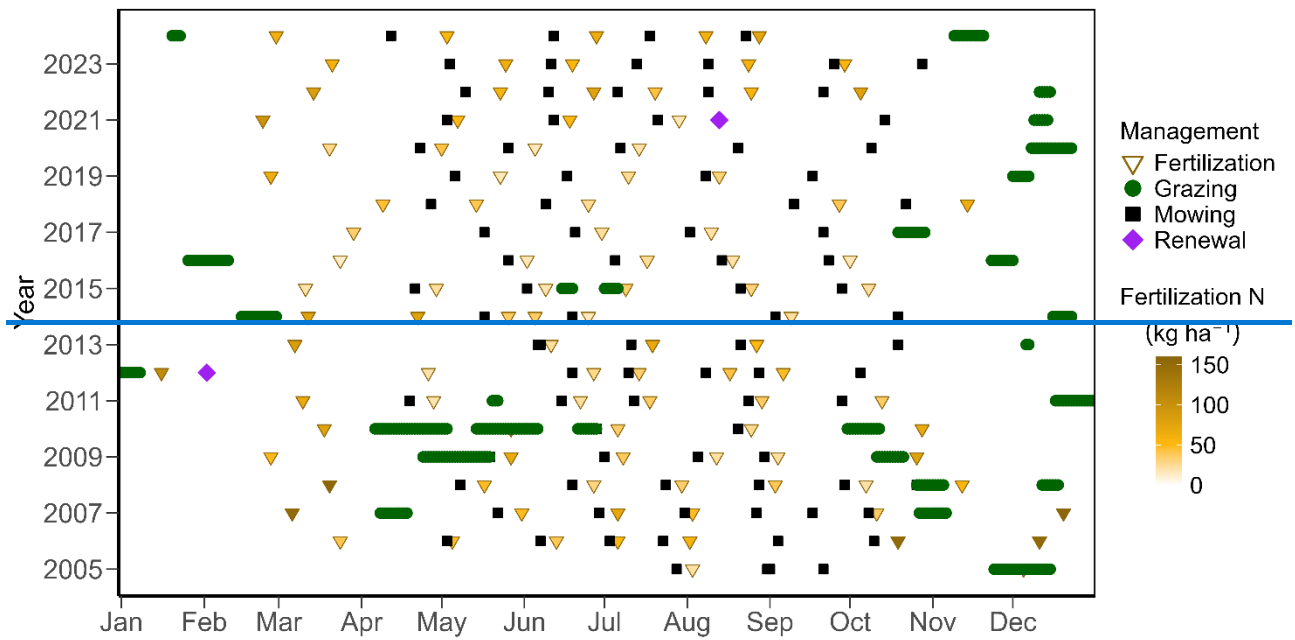


Figure A1. Annual cumulative sum of daily net ecosystem CO₂ exchange (NEE) for the years 2005 to 2024. Years during the N₂O mitigation experiment (2015 to 2020; see Methods and Feigenwinter et al., 2023b) are shown with dashed lines, years with sward renewals (2012 and 2021) are shown in thicker black and grey lines, respectively.



Figure



615 [Figure A2.A2](#). Major management events at the Chamau grassland site between July 2005 and December 2024. The x axis position of each point indicates the date of each event. Symbols represent different management activities: fertilization (brown triangles), mowing (black squares), grazing (green circles), and sward renewals (purple diamonds). Colours of fertilization triangles represent the amount of nitrogen inputs, with darker colours meaning higher inputs.

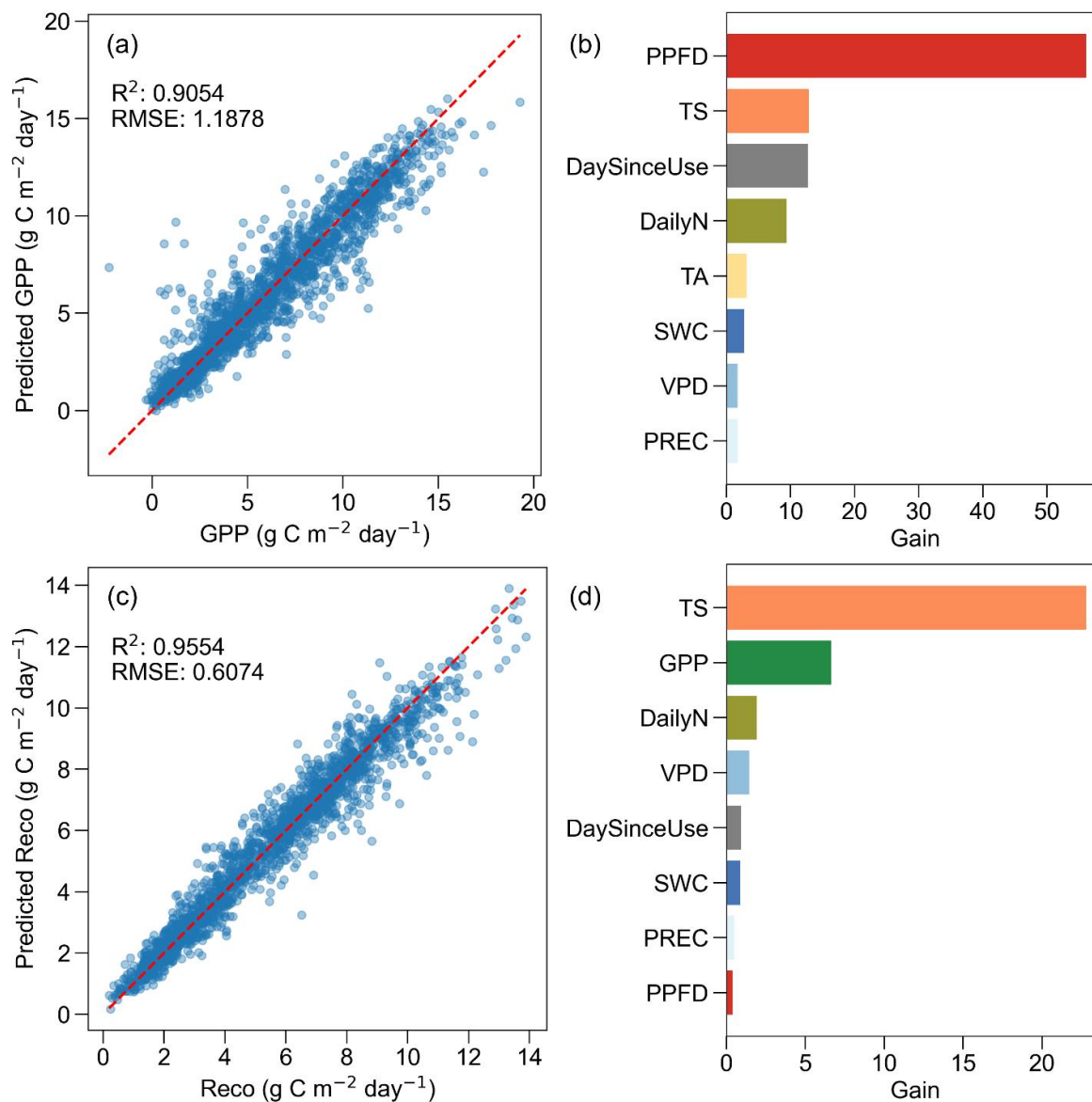


Figure A3. Performance and feature importance of XGBoost models for daily gross primary production (GPP) and ecosystem respiration (Reco). (a) Predicted versus actual GPP with model coefficient of determination (R^2) and root mean square error (RMSE) for the testing set, (b) feature importance (gain) for the GPP model, (c) predicted versus actual Reco with model R^2 and RMSE for the testing set, and (d) feature importance (gain) for the Reco model. In panels (a) and (c), red dashed lines represent 1:1 lines. In panels (b) and (d), higher gain values indicate higher importance of the features on model predictions. Features have the same colour code as in [Figure Fig. 4](#): photosynthetic photon flux density (PPFD, red), soil temperature (TS, orange), air temperature (TA, yellow), soil water content (SWC, dark blue), vapour pressure deficit (VPD, blue), precipitation (PREC, light blue), day since last mowing, grazing or renewal (DaySinceUse, grey), daily fertilizer nitrogen input (DailyN, moss green), and gross primary production (GPP, green).

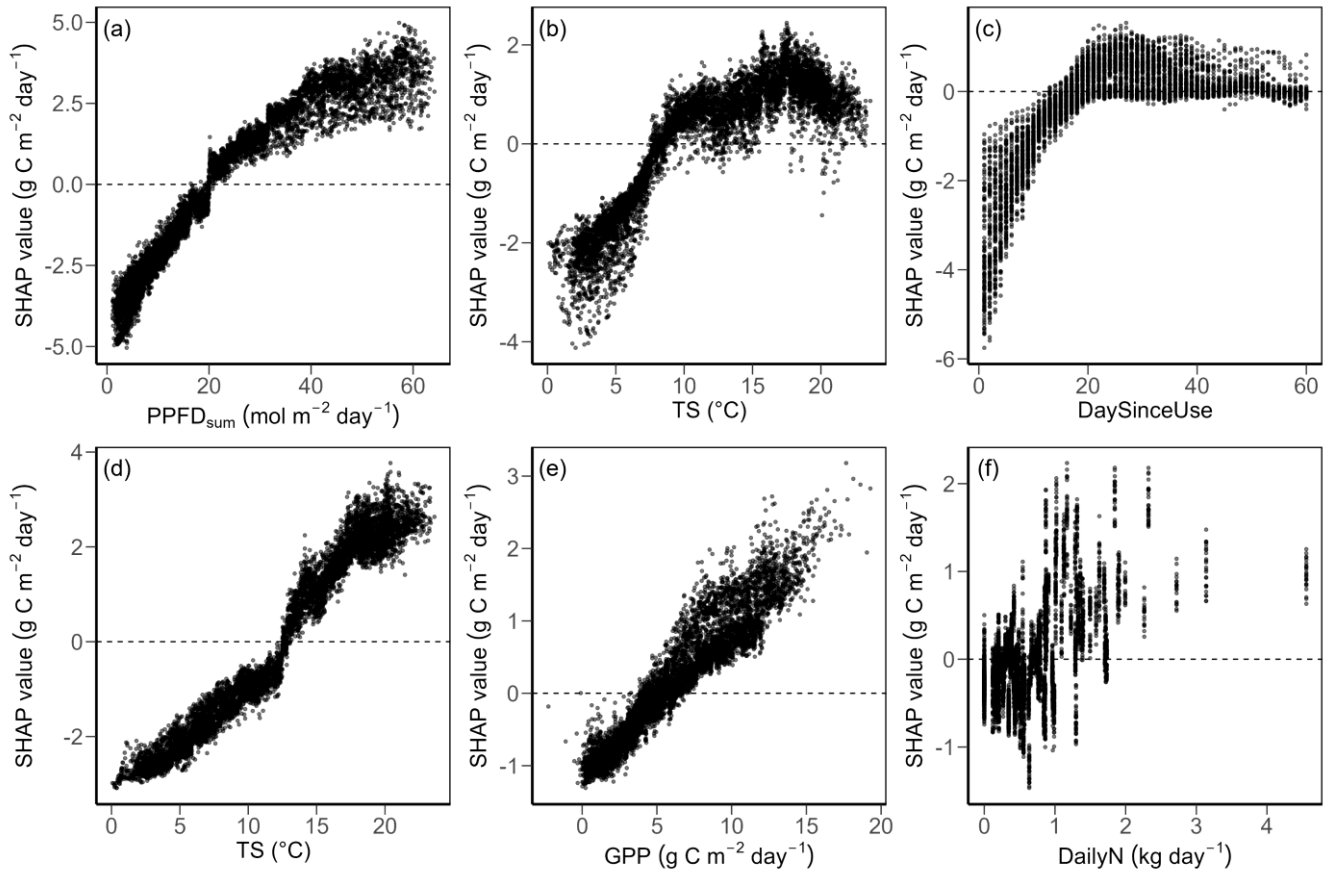
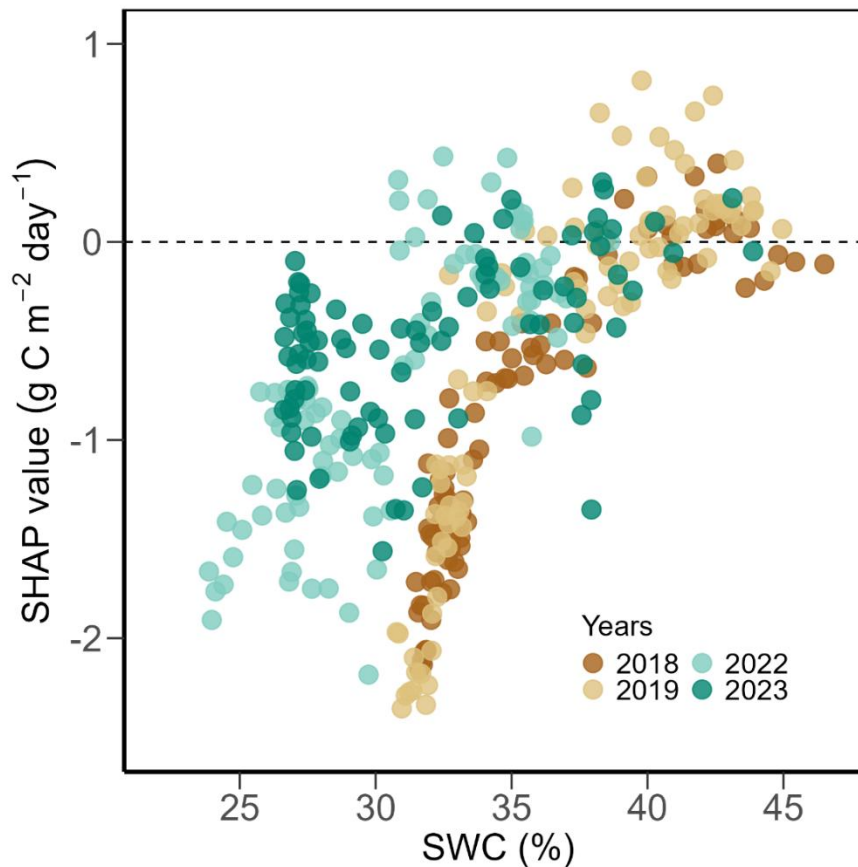


Figure A3. Partial dependence plots for the top three drivers of daily GPP (a to c) and Reco (d to f). (a) Total photosynthetic photon flux density (PPFD), (b) soil temperature (TS), and (c) day since last mowing, grazing or renewal (DaySinceUse, zoomed into first 60 days after management) vs. GPP. (d) Soil temperature (TS), (e) gross primary production (GPP), and (f) daily fertilization nitrogen input (DailyN) vs. Reco. SHAP values are the results of SHAP analysis 1 (Fig. 4). The mean prediction at SHAP value zero (dashed lines) corresponds to GPP of 6.1 g C m⁻² day⁻¹ and Reco of 5.3 g C m⁻² day⁻¹. Positive SHAP values represent positive effects of the drivers on GPP or Reco relative to the mean prediction, while negative values indicate negative effects from the mean prediction.

630



635

Figure A4. Partial dependence plot of SHAP values of volumetric soil water content (SWC) for predicted daily gross primary production (GPP) in the peak growing seasonseasons (June, July, August) during the years with extreme conditions 2018, 2019, 2022 and 2023 (see Fig. 2) from SHAP analysis 2 (Fig. 6). The mean prediction at SHAP value zero (dashed line) corresponds to a GPP of $9.7 \text{ g C m}^{-2} \text{ day}^{-1}$. Positive SHAP values represent positive impacteffects of SWC on GPP relative to the mean prediction, while negative values indicate negative impacteffects from the mean prediction. Different colours represent different years.

640

Code availability

The R and Python scripts used for the data analyses and visualizations are available upon request from the corresponding author. All scripts used in producing the PI dataset are available on GitHub (https://github.com/holukas/dataset_ch-cha_flux_product).

645 Data availability

Data used in this study will be openly available for download in the ETH Zurich Research Collection at <https://doi.org/10.3929/ethz-b-000745429> (Wang et al., 2025a; Preliminary link).

Author contribution

YW, IF, and NB: conceptualization of the study. YW, IF, and LH: data curation. YW: formal analysis, visualization, and writing (original draft preparation). IF and NB: supervision. AKG and NB: project administration. NB: funding acquisition. All authors: methodology and writing (reviewing and editing).

Competing interests

The authors declare that they have no conflict of interest.

Acknowledgements

The technical assistance for the maintenance of the eddy covariance station by Peter Plüss, Thomas Baur, Philip Meier, Patrick Koller, Florian Käslin, Paul Linwood, Markus Staudinger, Peter Ravelhofer, and Martin Rüegg is greatly acknowledged. Big thanks also go to all the scientists who were responsible for the Chamau site during the 20 years of this study: Matthias Zeeman, Werner Eugster, Lutz Merbold, Dennis Imer, and Kathrin Fuchs. We also thank Lukas Stocker and the staff from LBBZ Schluechthof team for managing the fields around the flux station. We acknowledge fruitful discussions with Wei Qiu, University of Washington, Seattle, USA, about machine learning models, in particular on SHAP analyses. AI tools (ChatGPT-4o, Grammarly, and DeepL) were used to improve writing and visualization. All outputs were critically reviewed by the authors to ensure accuracy and integrity.

Financial support

We acknowledge funding for the SNF projects InsuranceGrass (100018L_200918) and ICOS-CH Phase 3 (20FI20_198227). NB and YW are part of the SPEED2ZERO, a Joint Initiative co-financed by the ETH Board.

References

- Ammann, C., Flechard, C. R., Leifeld, J., Neftel, A., and Fuhrer, J.: The carbon budget of newly established temperate grassland depends on management intensity, *Agric. Ecosyst. Environ.*, 121, 5–20, <https://doi.org/10.1016/j.agee.2006.12.002>, 2007.
- Ammann, C., Neftel, A., Jocher, M., Fuhrer, J., and Leifeld, J.: Effect of management and weather variations on the greenhouse gas budget of two grasslands during a 10-year experiment, *Agric. Ecosyst. Environ.*, 292, 106814, <https://doi.org/10.1016/j.agee.2019.106814>, 2020.

- Anav, A., Friedlingstein, P., Beer, C., Ciais, P., Harper, A., Jones, C., Murray-Tortarolo, G., Papale, D., Parazoo, N. C., Peylin, P., Piao, S., Sitch, S., Viovy, N., Wiltshire, A., and Zhao, M.: Spatiotemporal patterns of terrestrial gross primary production: A review, *Rev. Geophys.*, 53, 785–818, <https://doi.org/10.1002/2015RG000483>, 2015.
- Aubinet, M., Vesala, T., and Papale, D. (Eds.): *Eddy Covariance: A Practical Guide to Measurement and Data Analysis*, Springer Netherlands, Dordrecht, <https://doi.org/10.1007/978-94-007-2351-1>, 2012.
- Bai, Y. and Cotrufo, M. F.: Grassland soil carbon sequestration: Current understanding, challenges, and solutions, *Science*, 377, 603–608, <https://doi.org/10.1126/science.abo2380>, 2022.
- 680 Barneze, A. S., Whitaker, J., McNamara, N. P., and Ostle, N. J.: Interactions between climate warming and land management regulate greenhouse gas fluxes in a temperate grassland ecosystem, *Sci. Total Environ.*, 833, 155212, <https://doi.org/10.1016/j.scitotenv.2022.155212>, 2022.
- Bengtsson, J., Bullock, J. M., Egoh, B., Everson, C., Everson, T., O'Connor, T., O'Farrell, P. J., Smith, H. G., and Lindborg, R.: Grasslands-more important for ecosystem services than you might think, *Ecosphere*, 10, e02582, <https://doi.org/10.1002/ecs2.2582>, 2019.
- 685 Bloor, J. M. G. and Bardgett, R. D.: Stability of above-ground and below-ground processes to extreme drought in model grassland ecosystems: Interactions with plant species diversity and soil nitrogen availability, *Perspect. Plant Ecol. Evol. Syst.*, 14, 193–204, <https://doi.org/10.1016/j.ppees.2011.12.001>, 2012.
- Breiman, L.: Random Forests, *Mach. Learn.*, 45, 5–32, <https://doi.org/10.1023/A:1010933404324>, 2001.
- 690 [Burba, G. G., McDermitt, D. K., Grelle, A., Anderson, D. J., and Xu, L.: Addressing the influence of instrument surface heat exchange on the measurements of CO₂ flux from open-path gas analyzers, *Global Change Biol.*, 14, 1854–1876, <https://doi.org/10.1111/j.1365-2486.2008.01606.x>, 2008.](https://doi.org/10.1111/j.1365-2486.2008.01606.x)
- Cai, W. and Prentice, I. C.: Recent trends in gross primary production and their drivers: analysis and modelling at flux-site and global scales, *Environ. Res. Lett.*, 15, 124050, <https://doi.org/10.1088/1748-9326/abc64e>, 2020.
- 695 ~~[CH2018: Climate scenarios for Switzerland, Technical Report, 2018.](#)~~
- ~~[CH2025: Climate CH2025 – Switzerland's Future Climate. Federal Office of Meteorology and Climatology MeteoSwiss, & ETH Zurich, 24 pp. <https://doi.org/10.18751/climate/scenarios/ch2025/brochure/1.0/en>, 2025.](#)~~
- 700 Chang, J., Ciais, P., Gasser, T., Smith, P., Herrero, M., Havlík, P., Obersteiner, M., Guenet, B., Goll, D. S., Li, W., Naipal, V., Peng, S., Qiu, C., Tian, H., Viovy, N., Yue, C., and Zhu, D.: Climate warming from managed grasslands cancels the cooling effect of carbon sinks in sparsely grazed and natural grasslands, *Nat. Commun.*, 12, 118, <https://doi.org/10.1038/s41467-020-20406-7>, 2021.

- Chen, T. and Guestrin, C.: XGBoost: A scalable tree boosting system, in: Proceedings of the 22nd ACM SIGKDD International Conference on Knowledge Discovery and Data Mining, New York, NY, USA, 785–794, <https://doi.org/10.1145/2939672.2939785>, 2016.
- 705 Craven, D., Isbell, F., Manning, P., Connolly, J., Bruelheide, H., Ebeling, A., Roscher, C., van Ruijven, J., Weigelt, A., Wilsey, B., Beierkuhnlein, C., de Luca, E., Griffin, J. N., Hautier, Y., Hector, A., Jentsch, A., Kreyling, J., Lanta, V., Loreau, M., Meyer, S. T., Mori, A. S., Naeem, S., Palmborg, C., Polley, H. W., Reich, P. B., Schmid, B., Siebenkäs, A., Seabloom, E., Thakur, M. P., Tilman, D., Vogel, A., and Eisenhauer, N.: Plant diversity effects on grassland productivity are robust to both nutrient enrichment and drought, *Philos. Trans. R. Soc. B Biol. Sci.*, 371, 20150277,
710 <https://doi.org/10.1098/rstb.2015.0277>, 2016.
- Davi, H., Dufrière, E., Francois, C., Le Maire, G., Loustau, D., Bosc, A., Rambal, S., Granier, A., and Moors, E.: Sensitivity of water and carbon fluxes to climate changes from 1960 to 2100 in European forest ecosystems, *Agric. For. Meteorol.*, 141, 35–56, <https://doi.org/10.1016/j.agrformet.2006.09.003>, 2006.
- 715 [Deventer, M. J., Roman, T., Bogoev, I., Kolka, R. K., Erickson, M., Lee, X., Baker, J. M., Millet, D. B., and Griffis, T. J.: Biases in open-path carbon dioxide flux measurements: Roles of instrument surface heat exchange and analyzer temperature sensitivity, *Agric. For. Meteorol.*, 296, 108216, <https://doi.org/10.1016/j.agrformet.2020.108216>, 2021.](https://doi.org/10.1016/j.agrformet.2020.108216)
- Drewer, J., Anderson, M., Levy, P. E., Scholtes, B., Helfter, C., Parker, J., Rees, R. M., and Skiba, U. M.: The impact of ploughing intensively managed temperate grasslands on N₂O, CH₄ and CO₂ fluxes, *Plant Soil*, 411, 193–208, <https://doi.org/10.1007/s11104-016-3023-x>, 2017.
- 720 Eugster, W. and Merbold, L.: Eddy covariance for quantifying trace gas fluxes from soils, *SOIL*, 1, 187–205, <https://doi.org/10.5194/soil-1-187-2015>, 2015.
- European Academies Science Advisory Council (Ed.): Regenerative agriculture in Europe: a critical analysis of contributions to European Union farm to fork and biodiversity strategies, EASAC Secretariat, Deutsche Akademie der Naturforscher Leopoldina - German National Academy of Sciences, Halle (Saale), 58 pp., 2022.
- 725 European Commission: Approved 28 CAP strategic plans (2023-2027), 2023.
- Eurostat: Share of main land types in utilised agricultural area (UAA) by NUTS 2 regions, 2020.
- Eurostat: Permanent agricultural grassland in Europe, 2023.
- [FAO: Climate-Smart Agriculture, https://www.fao.org/climate-smart-agriculture/en/, 2019.](https://www.fao.org/climate-smart-agriculture/en/)
- Federal Statistical Office (FSO): Die Landwirtschaftsflächen der Schweiz - 1985-2018, 2021.

- 730 Feigenwinter, I., Hörtnagl, L., Zeeman, M. J., Eugster, W., Fuchs, K., Merbold, L., and Buchmann, N.: Large inter-annual variation in carbon sink strength of a permanent grassland over 16 years: Impacts of management practices and climate, *Agric. For. Meteorol.*, 340, 109613, <https://doi.org/10.1016/j.agrformet.2023.109613>, 2023a.
- Feigenwinter, I., Hörtnagl, L., and Buchmann, N.: N₂O and CH₄ fluxes from intensively managed grassland: The importance of biological and environmental drivers vs. management, *Sci. Total Environ.*, 903, 166389, 735 <https://doi.org/10.1016/j.scitotenv.2023.166389>, 2023b.
- Feigenwinter, I., Wang, Y., Hörtnagl, L., Turco, F., Maier, R., and Buchmann, N.: High N₂O emissions after grassland destruction, In prep.
- Finger, R., Swinton, S. M., Benni, N. E., and Walter, A.: Precision farming at the nexus of agricultural production and the environment, *Annu. Rev. Resour. Econ.*, 11, 313–335, <https://doi.org/10.1146/annurev-resource-100518-093929>, 2019.
- 740 Finn, J. A., Suter, M., Haughey, E., Hofer, D., and Luscher, A.: Greater gains in annual yields from increased plant diversity than losses from experimental drought in two temperate grasslands, *Agric. Ecosyst. Environ.*, 258, 149–153, <https://doi.org/10.1016/j.agee.2018.02.014>, 2018.
- Fischer, E. M. and Knutti, R.: Detection of spatially aggregated changes in temperature and precipitation extremes, *Geophys. Res. Lett.*, 41, 547–554, <https://doi.org/10.1002/2013GL058499>, 2014.
- 745 Fu, Z., Ciais, P., Bastos, A., Stoy, P. C., Yang, H., Green, J. K., Wang, B., Yu, K., Huang, Y., Knohl, A., Šigut, L., Gharun, M., Cuntz, M., Arriga, N., Roland, M., Peichl, M., Migliavacca, M., Cremonese, E., Varlagin, A., Brümmer, C., Gourlez de la Motte, L., Fares, S., Buchmann, N., El-Madany, T. S., Pitacco, A., Vendrame, N., Li, Z., Vincke, C., Magliulo, E., and Koebsch, F.: Sensitivity of gross primary productivity to climatic drivers during the summer drought of 2018 in Europe, *Philos. Trans. R. Soc. B Biol. Sci.*, 375, 20190747, <https://doi.org/10.1098/rstb.2019.0747>, 2020.
- 750 Fuchs, K., Hörtnagl, L., Buchmann, N., Eugster, W., Snow, V., and Merbold, L.: Management matters: testing a mitigation strategy for nitrous oxide emissions using legumes on intensively managed grassland, *Biogeosciences*, 15, 5519–5543, <https://doi.org/10.5194/bg-15-5519-2018>, 2018.
- Gharun, M., Hörtnagl, L., Paul-Limoges, E., Ghiasi, S., Feigenwinter, I., Burri, S., Marquardt, K., Etzold, S., Zweifel, R., Eugster, W., and Buchmann, N.: Physiological response of Swiss ecosystems to 2018 drought across plant types and 755 elevation, *Philos. Trans. R. Soc. B Biol. Sci.*, 375, 20190521, <https://doi.org/10.1098/rstb.2019.0521>, 2020.
- Gilgen, A. K. and Buchmann, N.: Response of temperate grasslands at different altitudes to simulated summer drought differed but scaled with annual precipitation, *Biogeosciences*, 6, 2525–2539, <https://doi.org/10.5194/bg-6-2525-2009>, 2009.
- Gilmanov, T. G., Soussana, J. F., Aires, L., Allard, V., Ammann, C., Balzarolo, M., Barcza, Z., Bernhofer, C., Campbell, C. L., Cernusca, A., Cescatti, A., Clifton-Brown, J., Dirks, B. O. M., Dore, S., Eugster, W., Fuhrer, J., Gimeno, C., Gruenwald,

- 760 T., Haszpra, L., Hensen, A., Ibrom, A., Jacobs, A. F. G., Jones, M. B., Lanigan, G., Laurila, T., Lohila, A., G. Manca, Marcolla, B., Nagy, Z., Pilegaard, K., Pinter, K., Pio, C., Raschi, A., Rogiers, N., Sanz, M. J., Stefani, P., Sutton, M., Tuba, Z., Valentini, R., Williams, M. L., and Wohlfahrt, G.: Partitioning European grassland net ecosystem CO₂ exchange into gross primary productivity and ecosystem respiration using light response function analysis, *Agric. Ecosyst. Environ.*, 121, 93–120, <https://doi.org/10.1016/j.agee.2006.12.008>, 2007.
- 765 Gou, R., Chi, J., Liu, J., Luo, Y., Shekhar, A., Mo, L., and Lin, G.: Atmospheric water demand constrains net ecosystem production in subtropical mangrove forests, *J. Hydrol.*, 630, 130651, <https://doi.org/10.1016/j.jhydrol.2024.130651>, 2024.
- Grillakis, M. G.: Increase in severe and extreme soil moisture droughts for Europe under climate change, *Sci. Total Environ.*, 660, 1245–1255, <https://doi.org/10.1016/j.scitotenv.2019.01.001>, 2019.
- Hartmann, A. A., Barnard, R. L., Marhan, S., and Niklaus, P. A.: Effects of drought and N-fertilization on N cycling in two
770 grassland soils, *Oecologia*, 171, 705–717, <https://doi.org/10.1007/s00442-012-2578-3>, 2013.
- He, L., Chen, J. M., Croft, H., Gonsamo, A., Luo, X., Liu, J., Zheng, T., Liu, R., and Liu, Y.: Nitrogen availability dampens the positive impacts of CO₂ fertilization on terrestrial ecosystem carbon and water cycles, *Geophys. Res. Lett.*, 44, 11,590–11,600, <https://doi.org/10.1002/2017GL075981>, 2017.
- Heimsch, L., Lohila, A., Tuovinen, J.-P., Vekuri, H., Heinonsalo, J., Nevalainen, O., Korkiakoski, M., Liski, J., Laurila, T.,
775 and Kulmala, L.: Carbon dioxide fluxes and carbon balance of an agricultural grassland in southern Finland, *Biogeosciences*, 18, 3467–3483, <https://doi.org/10.5194/bg-18-3467-2021>, 2021.
- Heimsch, L., Vira, J., Fer, I., Vekuri, H., Tuovinen, J.-P., Lohila, A., Liski, J., and Kulmala, L.: Impact of weather and management practices on greenhouse gas flux dynamics on an agricultural grassland in Southern Finland, *Agric. Ecosyst. Environ.*, 374, 109179, <https://doi.org/10.1016/j.agee.2024.109179>, 2024.
- 780 Henwood, W. D.: An overview of protected areas in the temperate grasslands biome, *Parks*, 8, 3–8, 1998.
- Hermann, M., Wernli, H., and Röthlisberger, M.: Drastic increase in the magnitude of very rare summer-mean vapor pressure deficit extremes, *Nat. Commun.*, 15, 7022, <https://doi.org/10.1038/s41467-024-51305-w>, 2024.
- Hofer, D., Suter, M., ~~Haughey, E., Finn, J. A., Hoekstra, N. J.~~, Buchmann, N., and Lüscher, A.: ~~Yield~~Nitrogen status of ~~temperate functionally different~~ forage ~~grassland~~ species ~~is either largely resistant or resilient~~explains resistance to ~~experimental summersevere~~ drought, *J. Appl. Ecol.*, 53, 1023–1034 and post-drought overcompensation, *Agriculture, Ecosystems & Environment*, 236, 312–322, <https://doi.org/10.1111/1365-2664.12694>, <https://doi.org/10.1016/j.agee.2016.11.022>, 2017.
785
- Horst, T. W.: A simple formula for attenuation of eddy fluxes measured with first-order-response scalar sensors, *Bound.-Layer Meteorol.*, 82, 219–233, <https://doi.org/10.1023/A:1000229130034>, 1997.
- Hörtnagl, L.: diive v0.87.1, <https://doi.org/10.5281/zenodo.15648669>, 2025a.

- 790 Hörtnagl, L.: holukas/dataset_ch-cha_flux_product: FP2025.3, <https://doi.org/10.5281/zenodo.16058144>, 2025b.
- Hörtnagl, L., Barthel, M., Buchmann, N., Eugster, W., Butterbach-Bahl, K., Díaz-Pinés, E., Zeeman, M., Klumpp, K., Kiese, R., Bahn, M., Hammerle, A., Lu, H., Ladreiter-Knauss, T., Burri, S., and Merbold, L.: Greenhouse gas fluxes over managed grasslands in Central Europe, *Glob. Change Biol.*, 24, 1843–1872, <https://doi.org/10.1111/gcb.14079>, 2018.
- Hörtnagl, L., Feigenwinter, I., Wang, Y., Buchmann, N., Merbold, L., Zeeman, M., Fuchs, K., and Eugster, W.: Eddy
795 covariance ecosystem fluxes, meteorological data and detailed management information for the intensively managed grassland site Chamau in Switzerland, collected between 2005 and 2024: CH-CHA FP2025.3 (2005-2024), <https://doi.org/10.3929/ethz-b-000747025>, 2025.
- IPCC: Climate Change 2021 – The Physical Science Basis: Working Group I Contribution to the Sixth Assessment Report of the Intergovernmental Panel on Climate Change, Cambridge University Press, Cambridge,
800 <https://doi.org/10.1017/9781009157896>, 2023.
- Isbell, F., Craven, D., Connolly, J., Loreau, M., Schmid, B., Beierkuhnlein, C., Bezemer, T. M., Bonin, C., Bruelheide, H., de Luca, E., Ebeling, A., Griffin, J. N., Guo, Q., Hautier, Y., Hector, A., Jentsch, A., Kreyling, J., Lanta, V., Manning, P., Meyer, S. T., Mori, A. S., Naeem, S., Niklaus, P. A., Polley, H. W., Reich, P. B., Roscher, C., Seabloom, E. W., Smith, M. D., Thakur, M. P., Tilman, D., Tracy, B. F., van der Putten, W. H., van Ruijven, J., Weigelt, A., Weisser, W. W., Wilsey, B.,
805 and Eisenhauer, N.: Biodiversity increases the resistance of ecosystem productivity to climate extremes, *Nature*, 526, 574–577, <https://doi.org/10.1038/nature15374>, 2015.
- Jia, G., Shevliakova, E., Artaxo, P., De-Docoudré, N., Houghton, R., House, J., Kitajima, K., Lennard, C., Popp, A., Sirin, A., Sukumar, R., Verchot, L., and Sporre, M.: Land–Climate interactions, in: Special Report on Climate Change and Land, IPCC, 133–206, 2019.
- 810 Keenan, T. F., Gray, J., Friedl, M. A., Toomey, M., Bohrer, G., Hollinger, D. Y., Munger, J. W., O’Keefe, J., Schmid, H. P., Wing, I. S., Yang, B., and Richardson, A. D.: Net carbon uptake has increased through warming-induced changes in temperate forest phenology, *Nat. Clim. Change*, 4, 598–604, <https://doi.org/10.1038/nclimate2253>, 2014.
- Keenan, T. F., Luo, X., Stocker, B. D., De Kauwe, M. G., Medlyn, B. E., Prentice, I. C., Smith, N. G., Terrer, C., Wang, H., Zhang, Y., and Zhou, S.: A constraint on historic growth in global photosynthesis due to rising CO₂, *Nat. Clim. Change*, 13,
815 1376–1381, <https://doi.org/10.1038/s41558-023-01867-2>, 2023.
- Kendall, M. G.: Rank correlation methods, 2nd ed, Hafner Publishing Co., Oxford, England, vii, 196 pp., 1955.
- Knauer, J., Cuntz, M., Smith, B., Canadell, J. G., Medlyn, B. E., Bennett, A. C., Caldararu, S., and Haverd, V.: Higher global gross primary productivity under future climate with more advanced representations of photosynthesis, *Sci. Adv.*, 9, eadh9444, <https://doi.org/10.1126/sciadv.adh9444>, 2023.

- 820 Krebs, L., Hörtnagl, L., Scapucci, L., Gharun, M., Feigenwinter, I., and Buchmann, N.: Net ecosystem CO₂ exchange of a subalpine spruce forest in Switzerland over 26 years: Effects of phenology and contributions of abiotic drivers at daily time scales, *Glob. Change Biol.*, 31, e70371, <https://doi.org/10.1111/gcb.70371>, 2025.
- Li, H., Zhang, F., Li, J., Guo, X., Zhou, H., and Li, Y.: Differential responses of CO₂ and latent heat fluxes to climatic anomalies on two alpine grasslands on the northeastern Qinghai–Tibetan Plateau, *Sci. Total Environ.*, 900, 165863, 825 <https://doi.org/10.1016/j.scitotenv.2023.165863>, 2023a.
- Li, L., Fan, W., Kang, X., Wang, Y., Cui, X., Xu, C., Griffin, K. L., and Hao, Y.: Responses of greenhouse gas fluxes to climate extremes in a semiarid grassland, *Atmos. Environ.*, 142, 32–42, <https://doi.org/10.1016/j.atmosenv.2016.07.039>, 2016.
- Li, L., Zheng, Z., Biederman, J. A., Qian, R., Ran, Q., Zhang, B., Xu, C., Wang, F., Zhou, S., Che, R., Dong, J., Xu, Z., Cui, 830 X., Hao, Y., and Wang, Y.: Drought and heat wave impacts on grassland carbon cycling across hierarchical levels, *Plant Cell Environ.*, 44, 2402–2413, <https://doi.org/10.1111/pce.13767>, 2021.
- Li, Y., Korhonen, P., Kykkänen, S., Maljanen, M., Virkajärvi, P., and Shurpali, N. J.: Management practices during the renewal year affect the carbon balance of a boreal legume grassland, *Front. Sustain. Food Syst.*, 7, 1158250, <https://doi.org/10.3389/fsufs.2023.1158250>, 2023b.
- 835 [Lipper, L., Thornton, P., Campbell, B. M., Baedeker, T., Braimoh, A., Bwalya, M., Caron, P., Cattaneo, A., Garrity, D., Henry, K., Hottle, R., Jackson, L., Jarvis, A., Kossam, F., Mann, W., McCarthy, N., Meybeck, A., Neufeldt, H., Remington, T., Sen, P. T., Sessa, R., Shula, R., Tibu, A., and Torquebiau, E. F.: Climate-smart agriculture for food security, *Nat. Clim. Change*, 4, 1068–1072, <https://doi.org/10.1038/nclimate2437>, 2014.](#)
- Liu, Z., Chen, Z., Yang, M., Hao, T., Yu, G., Zhu, X., Zhang, W., Ma, L., Dou, X., Lin, Y., Luo, W., Han, L., Sun, M., 840 Chen, S., Dong, G., Gao, Y., Hao, Y., Jiang, S., Li, Y., Li, Y., Liu, S., Shi, P., Tan, J., Tang, Y., Xin, X., Zhang, F., Zhang, Y., Zhao, L., Zhou, L., and Zhu, Z.: Precipitation consistently promotes, but temperature oppositely drives carbon fluxes in temperate and alpine grasslands in China, *Agric. For. Meteorol.*, 344, 109811, <https://doi.org/10.1016/j.agrformet.2023.109811>, 2024.
- Lundberg, S. M. and Lee, S.-I.: A unified approach to interpreting model predictions, in: *Advances in Neural Information Processing Systems*, 2017. 845
- Lundberg, S. M., Erion, G., Chen, H., DeGrave, A., Prutkin, J. M., Nair, B., Katz, R., Himmelfarb, J., Bansal, N., and Lee, S.-I.: From local explanations to global understanding with explainable AI for trees, *Nat. Mach. Intell.*, 2, 56–67, <https://doi.org/10.1038/s42256-019-0138-9>, 2020.

- Madani, N., Parazoo, N. C., Kimball, J. S., Ballantyne, A. P., Reichle, R. H., Maneta, M., Saatchi, S., Palmer, P. I., Liu, Z.,
850 and Tagesson, T.: Recent amplified global gross primary productivity due to temperature increase Is offset by reduced
productivity due to water constraints, *AGU Adv.*, 1, e2020AV000180, <https://doi.org/10.1029/2020AV000180>, 2020.
- Maier, R., Hörtnagl, L., and Buchmann, N.: Greenhouse gas fluxes (CO₂, N₂O and CH₄) of pea and maize during two
cropping seasons: Drivers, budgets, and emission factors for nitrous oxide, *Sci. Total Environ.*, 849, 157541,
<https://doi.org/10.1016/j.scitotenv.2022.157541>, 2022.
- 855 Mann, H. B.: Nonparametric tests against trend, *Econometrica*, 13, 245–259, <https://doi.org/10.2307/1907187>, 1945.
- Merbold, L., Eugster, W., Stieger, J., Zahniser, M., Nelson, D., and Buchmann, N.: Greenhouse gas budget (CO₂, CH₄ and
N₂O) of intensively managed grassland following restoration, *Glob. Change Biol.*, 20, 1913–1928,
<https://doi.org/10.1111/gcb.12518>, 2014.
- MeteoSwiss: Klimabulletin Jahr 2022, 2023.
- 860 MeteoSwiss: Klimabulletin Jahr 2023, 2024.
- Molnar, C.: Interpreting Machine Learning Models with SHAP: A Guide with Python Examples and Theory on Shapley
Values, [Christoph Christoph](#) Molnar c/o MUCBOOK, Heidi Seibold, 208 pp., 2023.
- Moncrieff, J., Clement, R., Finnigan, J., and Meyers, T.: Averaging, detrending, and filtering of eddy covariance time series,
in: *Handbook of Micrometeorology: A Guide for Surface Flux Measurement and Analysis*, edited by: Lee, X., Massman, W.,
865 and Law, B., Springer Netherlands, Dordrecht, 7–31, https://doi.org/10.1007/1-4020-2265-4_2, 2005.
- Myneni, R. B., Keeling, C. D., Tucker, C. J., Asrar, G., and Nemani, R. R.: Increased plant growth in the northern high
latitudes from 1981 to 1991, *Nature*, 386, 698–702, <https://doi.org/10.1038/386698a0>, 1997.
- Norby, R. J., Warren, J. M., Iversen, C. M., Medlyn, B. E., and McMurtrie, R. E.: CO₂ enhancement of forest productivity
constrained by limited nitrogen availability, *Proc. Natl. Acad. Sci.*, 107, 19368–19373,
870 <https://doi.org/10.1073/pnas.1006463107>, 2010.
- [Pastorello, G., Trotta, C., Canfora, E., Chu, H., Christianson, D., Cheah, Y.-W., Poindexter, C., Chen, J., Elbashandy, A.,
Humphrey, M., Isaac, P., Polidori, D., Reichstein, M., Ribeca, A., van Ingen, C., Vuichard, N., Zhang, L., Amiro, B.,
Ammann, C., Arain, M. A., Ardö, J., Arkebauer, T., Arndt, S. K., Arriga, N., Aubinet, M., Aurela, M., Baldocchi, D., Barr,
A., Beamesderfer, E., Marchesini, L. B., Bergeron, O., Beringer, J., Bernhofer, C., Berveiller, D., Billesbach, D., Black, T.,
875 A., Blanken, P. D., Bohrer, G., Boike, J., Bolstad, P. V., Bonal, D., Bonnefond, J.-M., Bowling, D. R., Bracho, R., Brodeur,
J., Brümmer, C., Buchmann, N., Burban, B., Burns, S. P., Buysse, P., Cale, P., Cavagna, M., Cellier, P., Chen, S., Chini, I.,
Christensen, T. R., Cleverly, J., Collalti, A., Consalvo, C., Cook, B. D., Cook, D., Coursolle, C., Cremonese, E., Curtis, P. S.,
D’Andrea, E., da Rocha, H., Dai, X., Davis, K. J., Cinti, B. D., Grandcourt, A. de, Ligne, A. D., De Oliveira, R. C.,](#)

- 880 [Delpierre, N., Desai, A. R., Di Bella, C. M., Tommasi, P. di, Dolman, H., Domingo, F., Dong, G., Dore, S., Duce, P., Dufrêne, E., Dunn, A., Dušek, J., Eamus, D., Eichelmann, U., ElKhidir, H. A. M., Eugster, W., Ewenz, C. M., Ewers, B., Famulari, D., Fares, S., Feigenwinter, I., Feitz, A., Fensholt, R., Filippa, G., Fischer, M., Frank, J., Galvagno, M., et al.: The FLUXNET2015 dataset and the ONEFlux processing pipeline for eddy covariance data, *Sci. Data*, 7, 225, <https://doi.org/10.1038/s41597-020-0534-3>, 2020.](#)
- 885 Pedregosa, F., Varoquaux, G., Gramfort, A., Michel, V., Thirion, B., Grisel, O., Blondel, M., Prettenhofer, P., Weiss, R., Dubourg, V., Vanderplas, J., Passos, A., Cournapeau, D., Brucher, M., Perrot, M., and Duchesnay, É.: Scikit-learn: Machine Learning in Python, *J. Mach. Learn. Res.*, 12, 2825–2830, 2011.
- Peichl, M., Leahy, P., and Kiely, G.: Six-year stable annual uptake of carbon dioxide in intensively managed humid temperate grassland, *Ecosystems*, 14, 112–126, <https://doi.org/10.1007/s10021-010-9398-2>, 2011.
- 890 Piao, S., Friedlingstein, P., Ciais, P., Viovy, N., and Demarty, J.: Growing season extension and its impact on terrestrial carbon cycle in the Northern Hemisphere over the past 2 decades, *Glob. Biogeochem. Cycles*, 21, <https://doi.org/10.1029/2006GB002888>, 2007.
- Python Software Foundation: Python 3.11.11, Python Software Foundation, 2024.
- Qiu, W., Chen, H., Dincer, A. B., Lundberg, S., Kaeberlein, M., and Lee, S.-I.: Interpretable machine learning prediction of all-cause mortality, *Commun. Med.*, 2, 1–15, <https://doi.org/10.1038/s43856-022-00180-x>, 2022.
- 895 R Core Team: R: A Language and Environment for Statistical Computing, R Foundation for Statistical Computing, Vienna, Austria, 2024.
- Reichstein, M., Falge, E., Baldocchi, D., Papale, D., Aubinet, M., Berbigier, P., Bernhofer, C., Buchmann, N., Gilmanov, T., Granier, A., Grunwald, T., Havrankova, K., Ilvesniemi, H., Janous, D., Knohl, A., Laurila, T., Lohila, A., Loustau, D., Matteucci, G., Meyers, T., Miglietta, F., Ourcival, J.-M., Pumpanen, J., Rambal, S., Rotenberg, E., Sanz, M., Tenhunen, J., 900 Seufert, G., Vaccari, F., Vesala, T., Yakir, D., and Valentini, R.: On the separation of net ecosystem exchange into assimilation and ecosystem respiration: review and improved algorithm, *Glob. Change Biol.*, 11, 1424–1439, <https://doi.org/10.1111/j.1365-2486.2005.001002.x>, 2005.
- Reichstein, M., Bahn, M., Ciais, P., Frank, D., Mahecha, M. D., Seneviratne, S. I., Zscheischler, J., Beer, C., Buchmann, N., Frank, D. C., Papale, D., Rammig, A., Smith, P., Thonicke, K., van der Velde, M., Vicca, S., Walz, A., and Wattenbach, M.: 905 Climate extremes and the carbon cycle, *Nature*, 500, 287–295, <https://doi.org/10.1038/nature12350>, 2013.
- Richter, F., Suter, M., Lüscher, A., Buchmann, N., El Benni, N., Feola-Conz, R., Hartmann, M., Jan, P., and Klaus, V. H.: Effects of management practices on the ecosystem-service multifunctionality of temperate grasslands, *Nat. Commun.*, 15, 3829, <https://doi.org/10.1038/s41467-024-48049-y>, 2024.

- Rogger, J., Hörtnagl, L., Buchmann, N., and Eugster, W.: Carbon dioxide fluxes of a mountain grassland: Drivers, anomalies and annual budgets, *Agric. For. Meteorol.*, 314, 108801, <https://doi.org/10.1016/j.agrformet.2021.108801>, 2022.
- Roth, K.: Bodenkartierung und GIS-basierte Kohlenstoffinventur von Graslandboden: Untersuchungen an den ETH-Forschungsstationen Chamau und Fruebuel (ZG, Schweiz), Inst. Geogr. Univ. Zurich Master's Thesis, 2006.
- Schaub, S., Finger, R., Leiber, F., Probst, S., Kreuzer, M., Weigelt, A., Buchmann, N., and Scherer-Lorenzen, M.: Plant diversity effects on forage quality, yield and revenues of semi-natural grasslands, *Nat. Commun.*, 11, 768, <https://doi.org/10.1038/s41467-020-14541-4>, 2020.
- [Sabbatini, S., Mammarella, I., Arriga, N., Fratini, G., Graf, A., Hörtnagl, L., Ibrom, A., Longdoz, B., Mauder, M., Merbold, L., Metzger, S., Montagnani, L., Pitacco, A., Rebmann, C., Sedlák, P., Šigut, L., Vitale, D., and Papale, D.: Eddy covariance raw data processing for CO₂ and energy fluxes calculation at ICOS ecosystem stations, *Int. Agrophys.*, 32, 495–515, <https://doi.org/10.1515/intag-2017-0043>, 2018.](https://doi.org/10.1515/intag-2017-0043)
- Schaub, S., Finger, R., Buchmann, N., Steiner, V., and Klaus, V. H.: The costs of diversity: higher prices for more diverse grassland seed mixtures, *Environ. Res. Lett.*, 16, 094011, <https://doi.org/10.1088/1748-9326/ac1a9c>, 2021.
- Scherrer, S. C., Hirschi, M., Spirig, C., Maurer, F., and Kotlarski, S.: Trends and drivers of recent summer drying in Switzerland, *Environ. Res. Commun.*, 4, 025004, <https://doi.org/10.1088/2515-7620/ac4fb9>, 2022.
- Schils, R. L. M., Aarts, H. F. M., Bussink, D. W., Conijn, J. G., Corre, V. J., Dam, A. M. van, Hoving, I. E., Meer, H. G. van der, and Velthof, G. L.: Grassland renovation in the Netherlands; agronomic, environmental and economic issues, *Grassl. Resowing Grass-Arable Crops Rotat.*, 9–24, 2007.
- Schils, R. L. M., Bufe, C., Rhymer, C. M., Francksen, R. M., Klaus, V. H., Abdalla, M., Milazzo, F., Lellei-Kovács, E., Berge, H. ten, Bertora, C., Chodkiewicz, A., Dămățircă, C., Feigenwinter, I., Fernández-Rebollo, P., Ghiasi, S., Hejduk, S., Hiron, M., Janicka, M., Pellaton, R., Smith, K. E., Thorman, R., Vanwallegheem, T., Williams, J., Zavattaro, L., Kampen, J., Derkx, R., Smith, P., Whittingham, M. J., Buchmann, N., and Price, J. P. N.: Permanent grasslands in Europe: Land use change and intensification decrease their multifunctionality, *Agric. Ecosyst. Environ.*, 330, 107891, <https://doi.org/10.1016/j.agee.2022.107891>, 2022.
- Schwalm, C. R., Williams, C. A., Schaefer, K., Arneth, A., Bonal, D., Buchmann, N., Chen, J., Law, B. E., Lindroth, A., Luyssaert, S., Reichstein, M., and Richardson, A. D.: Assimilation exceeds respiration sensitivity to drought: A FLUXNET synthesis, *Glob. Change Biol.*, 16, 657–670, <https://doi.org/10.1111/j.1365-2486.2009.01991.x>, 2010.
- Sen, P. K.: Estimates of the regression coefficient based on Kendall's tau, *J. Am. Stat. Assoc.*, 63, 1379–1389, 1968.

- Shekhar, A., Buchmann, N., Humphrey, V., and Gharun, M.: More than three-fold increase in compound soil and air dryness across Europe by the end of 21st century, *Weather Clim. Extrem.*, 44, 100666, <https://doi.org/10.1016/j.wace.2024.100666>, 2024.
- 940 Shi, L., Lin, Z., Tang, S., Peng, C., Yao, Z., Xiao, Q., Zhou, H., Liu, K., and Shao, X.: Interactive effects of warming and managements on carbon fluxes in grasslands: A global meta-analysis, *Agric. Ecosyst. Environ.*, 340, 108178, <https://doi.org/10.1016/j.agee.2022.108178>, 2022.
- Soussana, J.-F., Loiseau, P., Vuichard, N., Ceschia, E., Balesdent, J., Chevallier, T., and Arrouays, D.: Carbon cycling and sequestration opportunities in temperate grasslands, *Soil Use Manag.*, 20, 219–230, <https://doi.org/10.1111/j.1475-2743.2004.tb00362.x>, 2004.
- 945 SUPER-G: PG Portraits, <https://www.super-g.eu/pg-portraits/>, 2018.
- Terrer, C., Jackson, R. B., Prentice, I. C., Keenan, T. F., Kaiser, C., Vicca, S., Fisher, J. B., Reich, P. B., Stocker, B. D., Hungate, B. A., Peñuelas, J., McCallum, I., Soudzilovskaia, N. A., Cernusak, L. A., Talhelm, A. F., Van Sundert, K., Piao, S., Newton, P. C. D., Hovenden, M. J., Blumenthal, D. M., Liu, Y. Y., Müller, C., Winter, K., Field, C. B., Viechtbauer, W.,
- 950 Van Lissa, C. J., Hoosbeek, M. R., Watanabe, M., Koike, T., Leshyk, V. O., Polley, H. W., and Franklin, O.: Nitrogen and phosphorus constrain the CO₂ fertilization of global plant biomass, *Nat. Clim. Change*, 9, 684–689, <https://doi.org/10.1038/s41558-019-0545-2>, 2019.
- Teuling, A. J., Seneviratne, S. I., Stöckli, R., Reichstein, M., Moors, E., Ciais, P., Luysaert, S., van den Hurk, B., Ammann, C., Bernhofer, C., Dellwik, E., Gianelle, D., Gielen, B., Grünwald, T., Klumpp, K., Montagnani, L., Moureaux, C.,
- 955 Sottocornola, M., and Wohlfahrt, G.: Contrasting response of European forest and grassland energy exchange to heatwaves, *Nat. Geosci.*, 3, 722–727, <https://doi.org/10.1038/ngeo950>, 2010.
- Wall, A. M., Campbell, D. I., Mudge, P. L., Rutledge, S., and Schipper, L. A.: Carbon budget of an intensively grazed temperate grassland with large quantities of imported supplemental feed, *Agric. Ecosyst. Environ.*, 281, 1–15, <https://doi.org/10.1016/j.agee.2019.04.019>, 2019.
- 960 Wall, A. M., Campbell, D. I., Mudge, P. L., and Schipper, L. A.: Temperate grazed grassland carbon balances for two adjacent paddocks determined separately from one eddy covariance system, *Agric. For. Meteorol.*, 287, 107942, <https://doi.org/10.1016/j.agrformet.2020.107942>, 2020.
- [Walter, A., Finger, R., Huber, R., and Buchmann, N.: Smart farming is key to developing sustainable agriculture, *PNAS*, 114, 6148–6150, <https://doi.org/10.1073/pnas.1707462114>, 2017.](https://doi.org/10.1073/pnas.1707462114)
- 965 Wang, N., Quesada, B., Xia, L., Butterbach-Bahl, K., Goodale, C. L., and Kiese, R.: Effects of climate warming on carbon fluxes in grasslands—A global meta-analysis, *Glob. Change Biol.*, 25, 1839–1851, <https://doi.org/10.1111/gcb.14603>, 2019.

- Wang, Y., Feigenwinter, I., Hörtnagl, L., Gilgen, A. K., and Buchmann, N.: Dataset including 20 years of daily CO₂ fluxes, meteorological data, and management information during regrowth periods from the intensively managed grassland site Chamau, <https://doi.org/10.3929/ethz-b-000745429>, 2025a.
- 970 Wang, Y., Klaus, V. H., Gilgen, A. K., and Buchmann, N.: Temperate grasslands under climate extremes: Effects of plant diversity on ecosystem services, *Agric. Ecosyst. Environ.*, 379, 109372, <https://doi.org/10.1016/j.agee.2024.109372>, 2025b.
- Webb, E. K., Pearman, G. I., and Leuning, R.: Correction of flux measurements for density effects due to heat and water vapour transfer, *Q. J. R. Meteorol. Soc.*, 106, 85–100, <https://doi.org/10.1002/qj.49710644707>, 1980.
- White, R. P., Murray, S., Rohweder, M., Prince, S., and Thompson, K.: Pilot Analysis of Global Ecosystems: Grassland
975 Ecosystems, World Resources Institute Washington, DC, USA, 2000.
- Wilczak, J. M., Oncley, S. P., and Stage, S. A.: Sonic Anemometer Tilt Correction Algorithms, *Bound.-Layer Meteorol.*, 99, 127–150, <https://doi.org/10.1023/A:1018966204465>, 2001.
- Winck, B., Klumpp, K., and Bloor, J. M. G.: Interactive effects of management and temperature anomalies on CO₂ fluxes recorded over 18 years in a temperate upland grassland system, *Agric. For. Meteorol.*, 362, 110343,
980 <https://doi.org/10.1016/j.agrformet.2024.110343>, 2025.
- Winck, B. R., Bloor, J. M. G., and Klumpp, K.: Eighteen years of upland grassland carbon flux data: reference datasets, processing, and gap-filling procedure, *Sci. Data*, 10, 311, <https://doi.org/10.1038/s41597-023-02221-z>, 2023.
- Winkler, K., Fuchs, R., Rounsevell, M., and Herold, M.: Global land use changes are four times greater than previously estimated, *Nat. Commun.*, 12, 2501, <https://doi.org/10.1038/s41467-021-22702-2>, 2021.
- 985 Wohlfahrt, G., Hammerle, A., Haslwanter, A., Bahn, M., Tappeiner, U., and Cernusca, A.: Seasonal and inter-annual variability of the net ecosystem CO₂ exchange of a temperate mountain grassland: Effects of weather and management, *J. Geophys. Res. Atmospheres*, 113, D08110, <https://doi.org/10.1029/2007JD009286>, 2008.
- Woo, D. K., Riley, W. J., Grant, R. F., and Wu, Y.: Site-specific field management adaptation is key to feeding the world in the 21st century, *Agric. For. Meteorol.*, 327, 109230, <https://doi.org/10.1016/j.agrformet.2022.109230>, 2022.
- 990 [World Bank: Climate-Smart Agriculture, https://www.worldbank.org/en/topic/climate-smartagriculture, 2024.](https://www.worldbank.org/en/topic/climate-smartagriculture)
- Wutzler, T., Lucas-Moffat, A., Migliavacca, M., Knauer, J., Sickel, K., Šigut, L., Menzer, O., and Reichstein, M.: Basic and extensible post-processing of eddy covariance flux data with REddyProc, *Biogeosciences*, 15, 5015–5030, <https://doi.org/10.5194/bg-15-5015-2018>, 2018.
- Xia, J., Niu, S., Ciais, P., Janssens, I. A., Chen, J., Ammann, C., Arain, A., Blanken, P. D., Cescatti, A., Bonal, D.,
995 Buchmann, N., Curtis, P. S., Chen, S., Dong, J., Flanagan, L. B., Frankenberg, C., Georgiadis, T., Gough, C. M., Hui, D., Kiely, G., Li, J., Lund, M., Magliulo, V., Marcolla, B., Merbold, L., Montagnani, L., Moors, E. J., Olesen, J. E., Piao, S.,

- Raschi, A., Roupsard, O., Suyker, A. E., Urbaniak, M., Vaccari, F. P., Varlagin, A., Vesala, T., Wilkinson, M., Weng, E., Wohlfahrt, G., Yan, L., and Luo, Y.: Joint control of terrestrial gross primary productivity by plant phenology and physiology, *Proc. Natl. Acad. Sci.*, 112, 2788–2793, <https://doi.org/10.1073/pnas.1413090112>, 2015.
- 1000 Xu, C., McDowell, N. G., Fisher, R. A., Wei, L., Sevanto, S., Christoffersen, B. O., Weng, E., and Middleton, R. S.: Increasing impacts of extreme droughts on vegetation productivity under climate change, *Nat. Clim. Change*, 9, 948–953, <https://doi.org/10.1038/s41558-019-0630-6>, 2019.
- Zeeman, M. J., Hiller, R., Gilgen, A. K., Michna, P., Plüss, P., Buchmann, N., and Eugster, W.: Management and climate impacts on net CO₂ fluxes and carbon budgets of three grasslands along an elevational gradient in Switzerland, *Agric. For. Meteorol.*, 150, 519–530, <https://doi.org/10.1016/j.agrformet.2010.01.011>, 2010.
- 1005 Zhou, G., Luo, Q., Chen, Y., He, M., Zhou, L., Frank, D., He, Y., Fu, Y., Zhang, B., and Zhou, X.: Effects of livestock grazing on grassland carbon storage and release override impacts associated with global climate change, *Glob. Change Biol.*, 25, 1119–1132, <https://doi.org/10.1111/gcb.14533>, 2019.
- Zscheischler, J., Reichstein, M., Harmeling, S., Rammig, A., Tomelleri, E., and Mahecha, M. D.: Extreme events in gross primary production: a characterization across continents, *Biogeosciences*, 11, 2909–2924, <https://doi.org/10.5194/bg-11-2909-2014>, 2014.
- 1010